

1

2 **Supplementary Information for**

3 **Can Auxiliary Indicators Improve COVID-19 Forecasting and Hotspot Prediction?**

4 **Daniel J. McDonald, Jacob Bien, Alden Green, Addison J. Hu, Nat DeFries, Sangwon Hyun, Natalia L. Oliveira, James**
5 **Sharpnack, Jingjing Tang, Robert Tibshirani, Valerie Ventura, Larry Wasserman, and Ryan J. Tibshirani**

6 **Daniel J. McDonald.**
7 **E-mail: daniel@stat.ubc.ca**

8 **This PDF file includes:**

9 Supplementary text
10 Figs. S1 to S27 (not allowed for Brief Reports)
11 Table S1 (not allowed for Brief Reports)
12 Legends for Dataset S1 to S4
13 SI References

14 **Other supplementary materials for this manuscript include the following:**

15 Datasets S1 to S4

Supporting Information Text

1. Examining the relative advantage of using finalized rather than vintage data

The goal of this section is to quantify the effect of not properly accounting for the question of “what was known when” in performing retrospective evaluations of forecasters. Figures S1 and S2 show what Figures 3 and 4 in the main paper would have looked like if we had simply trained all models using the finalized data rather than using vintage data. This comparison can be seen more straightforwardly in Figures S3 and S4, which show the ratio in performance between the vintage and finalized versions. When methods are given the finalized version of the data rather than the version available at the time that the forecast would have been made, all methods appear (misleadingly) to have better performance than they would have had if run prospectively. For example, for forecasting case rates 7-days ahead, the WIS of all methods is at least 8% larger than what would have been achieved using finalized data. This effect diminishes as the forecasting horizon increases, reflecting the fact that longer-horizon forecasters rely less heavily on recent data than very short-horizon forecasters. Crucially, some methods are “helped” more than others by the less scrupulous retrospective evaluation, underscoring the difficulty of avoiding misleading conclusions when performing retrospective evaluations of forecasters.

CHNG-CLI (and, to a lesser extent, the other claims-based signals) is the most affected by this distinction, reflecting the latency in claims-based reporting. This underscores the importance of efforts to provide “nowcasts” for claims signals (which corresponds to a 0-ahead forecast of what the claims signal’s value will be once all data has been collected). Looking at the CHNG-CLI and DV-CLI curves in Figure S1, we can see that they perform very similarly when trained on the finalized data. This is reassuring because they are, in principle, measuring the same thing (namely, the percentage of outpatient visits that are primarily about COVID-related symptoms). The substantial difference in their curves in Figure 3 of the main paper must therefore reflect their having very different backfill profiles.

While using finalized rather than vintage data affects DV-CLI the least for forecasting, it is one of the most affected methods for the hotspot problem. This is a reminder that the forecasting and hotspot problems are fundamentally distinct. For example, the hotspot problem does not measure the ability to distinguish between flat and downward trends.

Even the AR model is affected by this distinction, reflecting the fact that the case rates themselves (i.e., the response values) are also subject to revision. The forecasters based on indicators are thus affected both by revisions to the indicators and by revisions to the case rates. In the case of the Google-AA model, in which we only used finalized values for the Google-AA indicator, the difference in performance can be wholly attributed to revisions of case rates.

2. Aggregating with geometric mean

In this section, we consider using the geometric mean instead of the arithmetic mean when aggregating the weighted interval score (WIS) across location-time pairs. There are three reasons why using the geometric mean may be desirable.

1. WIS is right-skewed, being bounded below by zero and having occasional very large values. Figure S5 illustrates that the densities appear roughly log-Gaussian. The geometric mean is a natural choice in such a context since the relative ordering of forecasters is determined by the arithmetic mean of the *logarithm* of their WIS values.
2. In the main paper, we report the ratio of the mean WIS of a forecaster to the mean WIS of the baseline forecaster. Another choice could be to take the mean of the ratio of WIS values for the two methods. This latter choice would penalize a method less for doing poorly where the baseline forecaster also does poorly. Using instead the geometric mean makes the order of aggregation and scaling immaterial since the ratio of geometric means is the same as the geometric mean of ratios.
3. If one imagines that a forecaster’s WIS is composed of multiplicative space-time effects $S_{\ell,t}$ shared across all forecasters, i.e. $\text{WIS}(F_{\ell,t,f}, Y_{\ell,t}) = S_{\ell,t} E_{f,t}$ with $E_{f,t}$ a forecaster-specific error, then taking the ratio of two forecasters’ geometric mean WIS values will effectively cancel these space-time effects.

Figure S6 uses the geometric mean for aggregation. Comparing this with Figure 3 of the main paper, we see that the main conclusions are largely unchanged; however, CHNG-CLI now appears better than AR. This behavior would be expected if CHNG-CLI’s poor performance is attributable to a relatively small number of large errors (as opposed to a large number of moderate errors). Indeed, Figure 5 of the main paper further corroborates this, in which we see the heaviest left tails occurring for CHNG-CLI.

3. Statistical significance

In the Introduction of the main paper, we give some reasons that we avoid making formal statements about statistical significance, preferring instead to examine the stability of our results in different contexts. There are strong reasons to avoid model-based significance tests because the necessary assumptions about stationarity, independence, and the model being true (or at least approximately true) are certainly violated. With those caveats in mind, we undertake two relatively assumption-lean investigations in this section. The first is a sign-test for whether the difference between the AR model’s relative WIS and each other model’s relative WIS is centered at zero. By “relative WIS” we mean scaled by the strawman as displayed in Figure 3. To mitigate the dependence across time (which intuitively seems to matter more than that across space), we computed these tests in a stratified way, where for each forecast date we run a sign test on the scaled errors between two models over all 440

counties. The results are plotted as histograms in Figure S7. In this case, we use the total relative WIS over all aheads, but the histograms are largely similar for individual target horizons. If there were no difference, we would expect to see a uniform distribution. However, for all indicator-assisted models, we see many more small P -values than would be expected if the null hypothesis (that the AR model is better) were true.

Another relatively assumption-lean method of testing for differences in forecast accuracy is the Diebold-Mariano test (1–3). Essentially, the differences between forecast losses are assumed to have a constant mean and a covariance that depends on time. Under these conditions, the asymptotic distribution for the standardized mean of the differences is limiting normal provided that a heteroskedasticity and autocorrelation robust estimate of the variance is used. Using the loss as weighted interval score across all HRRs and horizons (7 to 21 days ahead), we perform the DM test using both the mean relative to the strawman (as reported in the manuscript) and the geometric mean relative to the strawman as described above. The first two rows of Table S1 displays P -values for the test that the indicator-assisted model is no-better than the AR model. Only the CHNG-CLI model’s P -value exceeds conventional statistical significance thresholds.

4. Bootstrap results

As explained in Section 2.B. of the main paper, a (somewhat cynical) hypothesis for why we see benefits in forecasting and hotspot prediction is that the indicators are not actually providing useful information but they are instead acting as a sort of “implicit regularization,” leading to shrinkage on the autoregressive coefficients and therefore to less volatile predictions. To investigate this hypothesis, we consider fitting “noise features” that in truth should have zero coefficients. Recall (from the main paper) that at each forecast date, we train a model on 6,426 location-time pairs. Indicator models are based on six features, corresponding to the three autoregressive terms and the three lagged indicator values. To form noise indicator features, we replace their values with those from a randomly chosen time-space pair (while keeping the autoregressive features fixed). In particular, at each location ℓ and time t , for the forecasting task we replace the triplet $(X_{\ell,t}, X_{\ell,t-7}, X_{\ell,t-14})$ in Eq. (3) of the main paper with the triplet $(X_{\ell^*,t^*}, X_{\ell^*,t^*-7}, X_{\ell^*,t^*-14})$, where (ℓ^*, t^*) is a location-time pair sampled with replacement from the 6,426 location-time pairs. Likewise in the hotspot prediction task, we replace the triplet $(X_{\ell,t}^{\Delta}, X_{\ell,t-7}^{\Delta}, X_{\ell,t-14}^{\Delta})$ in Eq. (5) of the main paper with $(X_{\ell^*,t^*}^{\Delta}, X_{\ell^*,t^*-7}^{\Delta}, X_{\ell^*,t^*-14}^{\Delta})$. Figures S8–S10 show the results. No method exhibits a noticeable performance gain over the AR method, leading us to dismiss the implicit regularization hypothesis.

5. Upswings and Downswings

In this section we provide extra details about the upswing / flat / downswing analysis described in the main text. Figure S11 shows the overall results, examining the average difference $\text{WIS}(\text{AR}) - \text{WIS}(F)$ in period. Figure S13 shows the same information for the hotspot task. On average, during downswings and flat periods, the indicator-assisted models have lower classification error and higher log likelihood than the AR model. For hotspots, both Google-AA and CTIS-CLIC perform better than the AR model during upswings, in contrast to the forecasting task, where only Google-AA improves. For a related analysis, Figure S15 shows histograms of the Spearman correlation (Spearman’s ρ , a rank-based measure of association) between the $\text{WIS}(F)/\text{WIS}(\text{AR})$ and the magnitude of the swing. Again we see that case rate increases are positively related to diminished performance of the indicator models.

One hypothesis for diminished relative performance during upswings is that the AR model tends to overpredict downswings and underpredict upswings. Adding indicators appears to help avoid this behavior on the downswing but not as much on upswings. Figure S16 shows the correlation between $\text{WIS}(\text{AR}) - \text{WIS}(F)$ and the difference of their median forecasts. During downswings, this correlation is large, implying that improved relative performance of F is related to making lower forecasts than the AR model. The opposite is true during upswings. This is largely to be expected. However, the relationship attenuates in flat periods and during upswings. That is, when performance is better in those cases, it may be due to other factors than simply making predictions in the correct direction, for example, narrower confidence intervals.

6. Leadingness and laggingness

In Section 2.D of the main text, we discuss the extent to which the indicators are leading or lagging case rates during different periods. To define the amount of leadingness or laggingness at location ℓ , we use the cross correlation function (CCF) between the two time series. The $\text{CCF}_{\ell}(a)$ of an indicator X_{ℓ} and case rates Y_{ℓ} is defined as their Pearson correlation where X_{ℓ} has been aligned with the values of Y_{ℓ} that occurred a days earlier. Thus, for any $a > 0$, $\text{CCF}_{\ell}(a) > 0$ indicates that $Y_{\ell,t}$ is moving together with $X_{\ell,t+a}$. In this case we say that X_{ℓ} is lagging Y_{ℓ} . For $a < 0$, $\text{CCF}_{\ell}(a) > 0$ means that $Y_{\ell,t}$ is positively correlated with $X_{\ell,t-a}$, so we say that X_{ℓ} leads Y_{ℓ} .

Figure S17 shows the standardized signals for the HRR containing Charlotte, North Carolina, from August 1, 2020 until the end of September. These are the same signals shown in Figure 1 in the manuscript but using finalized data. To define “leadingness” we compute $\text{CCF}_{\ell}(a)$ (as implemented with the R function `ccf()`) for each $a \in \{-15, \dots, 15\}$ using the 56 days leading up to the target date. This is the same amount of data used to train the forecasters: 21 days of training data, 21 days to get the response at $a = 21$, and 14 days for the longest lagged value. The orange dashed horizontal line represents the 95% significance threshold for correlations based on 56 observations. Any correlations larger in magnitude than this value are considered statistically significant under the null hypothesis of no relationship. We define leadingness to be the sum of the significant correlations that are leading (those above the dashed line with $a < 0$) while laggingness is the same but for $a > 0$.

In the figure, there are three significant correlations on the “leading” side (at $a = -5, -4, -3$), so leadingness will be the sum of those values while laggingness is 0: on September 28 in Charlotte, DV-CLI is leading cases leading but not lagging.

Figure S18 shows the correlation between laggingness and the difference in indicator WIS and AR WIS. Unlike leadingness (Figure 5 in the manuscript) there is no obvious relationship that holds consistently across indicators. This is heartening as laggingness should not aid forecasting performance. On the other hand, if an indicator is more lagging than it is leading, this may suggest diminished performance. Figure S19 shows the correlation of the difference in leadingness and laggingness with the difference in WIS. The pattern here is largely similar to the pattern in leadingness described in the manuscript: the relationship is strongest in down periods and weakest in up periods with the strength diminishing as we move from down to flat to up for all indicators.

In calculating the CCF and the associated leadingness and laggingness scores, we have used the finalized data, and we look at the behavior at the target date of the forecast. That is we are using the same data to evaluate predictive accuracy as to determine leadingness and laggingness. It should be noted that the leadingness of the indicator at the time the model is trained may also be important. Thus, we could calculate separate leadingness and laggingness scores for the trained model and for the evaluation data and examine their combination in some way. We do not pursue this combination further and leave this investigation for future work.

7. Examining data in 2021

In this section, we investigate the sensitivity of the results to the period over which we train and evaluate the models. In the main paper, we end all evaluation on December 31, 2020. Figures S20–S22 show how the results would differ if we extended this analysis through March 31, 2021. Comparing Figure S20 to Figure 3 of the main paper, one sees that as ahead increases most methods now improve relative to the baseline forecaster. When compared to other methods, CHNG-CLI appears much better than it had previously; however, all forecasters other than CHNG-COVID and DV-CLI are performing less well relative to the baseline than before. These changes are likely due to the differing nature of the pandemic in 2021, with flat and downward trends much more common than upward trajectories. Indeed, the nature of the hotspot prediction problem is quite different in this period. With a 21-day training window, it is common for there to be many fewer hotspots in training.

8. Examining accumulated error over time and space

Following the suggestion of an anonymous reviewer, we investigate two disaggregated versions of the main forecasting result shown in Figure 3 on the manuscript. The first (Figure S23) displays the cumulative error (summed over all horizons) of each forecaster divided by the cumulative error of the baseline. This perspective should illustrate how the models perform over time, drawing attention to any nonstationary behavior. During the initial increase in cases in July 2020, CTIS-CLIIC and Google-AA gain a lot relative to the AR model. All the indicators do much better than the AR model during the following downturn (the ebb of the second wave). The AR model actually improves over the indicators in October 2020, before losing a bit in late November.

Figure S25 examines the spatial behavior over the entire period of the indicator-assisted models relative to the AR. For ease of comparison, we show the percent improvement in each HRR. Negative numbers (blue) mean that the indicator helped while positives (red) mean that the indicator hurt forecasting performance. The clear pattern is that in most HRRs, the indicators improved performance, though usually by small amounts (2.5%–10%). In some isolated HRRs, performance was markedly worse, though there does not appear to be any particular pattern to these locations.

9. Comparisons to state-of-the-art forecasters

Since mid-July 2020, a number of forecasting teams (48 in total) have submitted 1–4 week ahead state-level case forecasts to the COVID19 Forecast Hub (4). To compare those forecasts to those created in this paper, we selected only those forecasters who submitted at least 300 forecasts for the 2-week-ahead target before January 1, 2021 (approximately 1 forecast for each state for 6 weeks). This left 32 forecasters, one of which, the COVIDhub-4-week-ensemble, was an exact duplicate of another. To make the comparison fair, we scaled by the COVIDhub-baseline as in Figure 3 of the manuscript. Figure S26 shows all submitted forecasts (available 7, 14, and 21 days ahead) overlaid on Figure 3. We have highlighted the COVIDhub-ensemble in light blue for comparison. All the models developed in this paper beat the baseline, and would rank in the top 8 of 31 submitted forecasts over this period.

A more fair comparison that directly adjusts for spatiotemporal difficulty is to use the geometric mean scaled by the baseline. This is the same idea shown in S6. We have also remade this figure overlaying submitted forecasts available on the Forecast Hub. It occasionally happens that a submitted forecast achieved a WIS of 0, so in this case we use the WIS+1 rather than WIS for all forecasters. The result is shown in S27. By this metric, the methods employed in this paper would rank in the top 2, beating the COVIDhub-ensemble at all forecast horizons. The improvement of the best indicator assisted model over the AR model is roughly the same as the improvement of the AR model over the COVIDhub-ensemble.

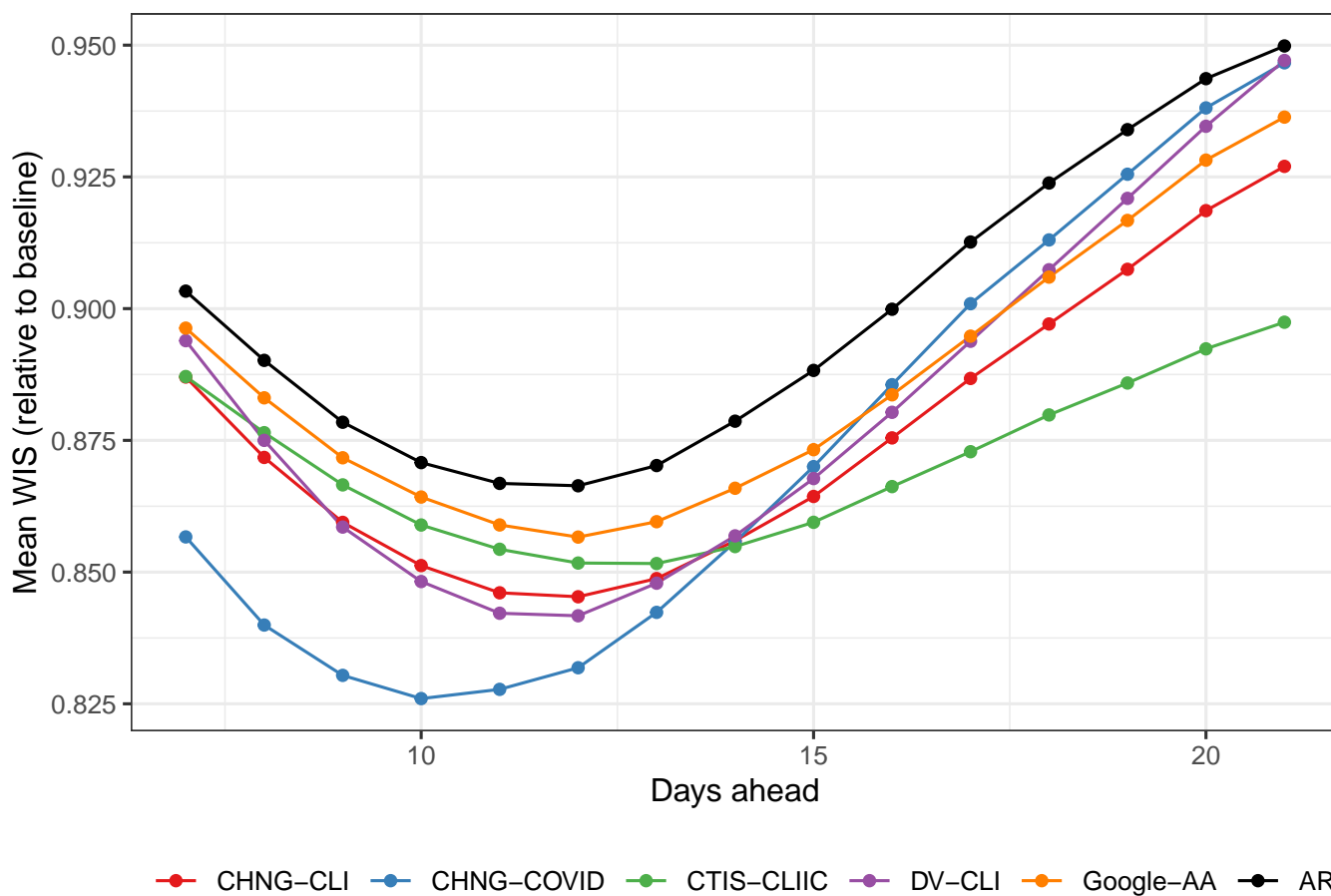


Fig. S1. Forecasting performance using finalized data. Compare to Figure 3 in the manuscript.

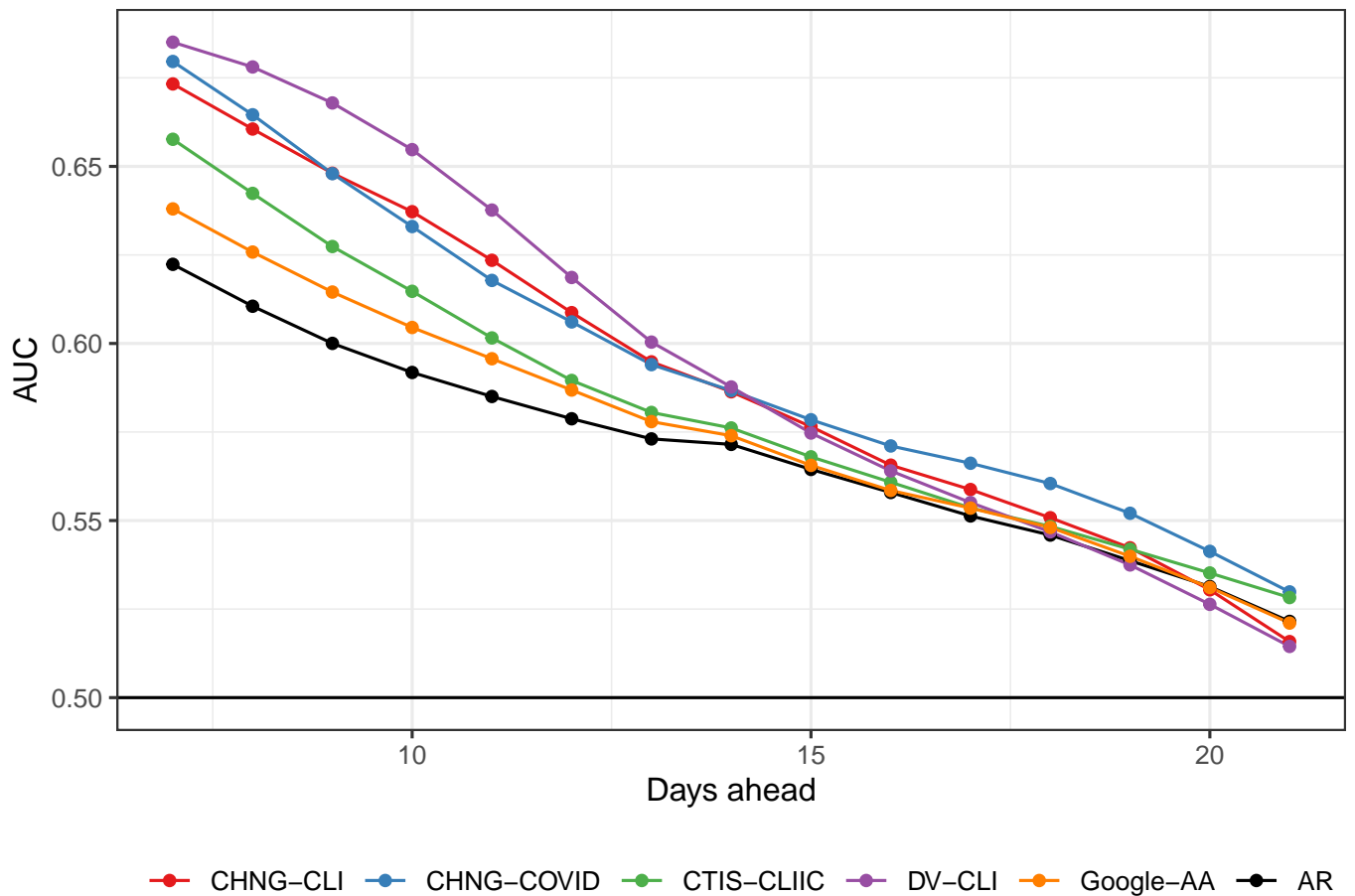


Fig. S2. Hotspot prediction performance using finalized data. Compare to Figure 4 in the manuscript.

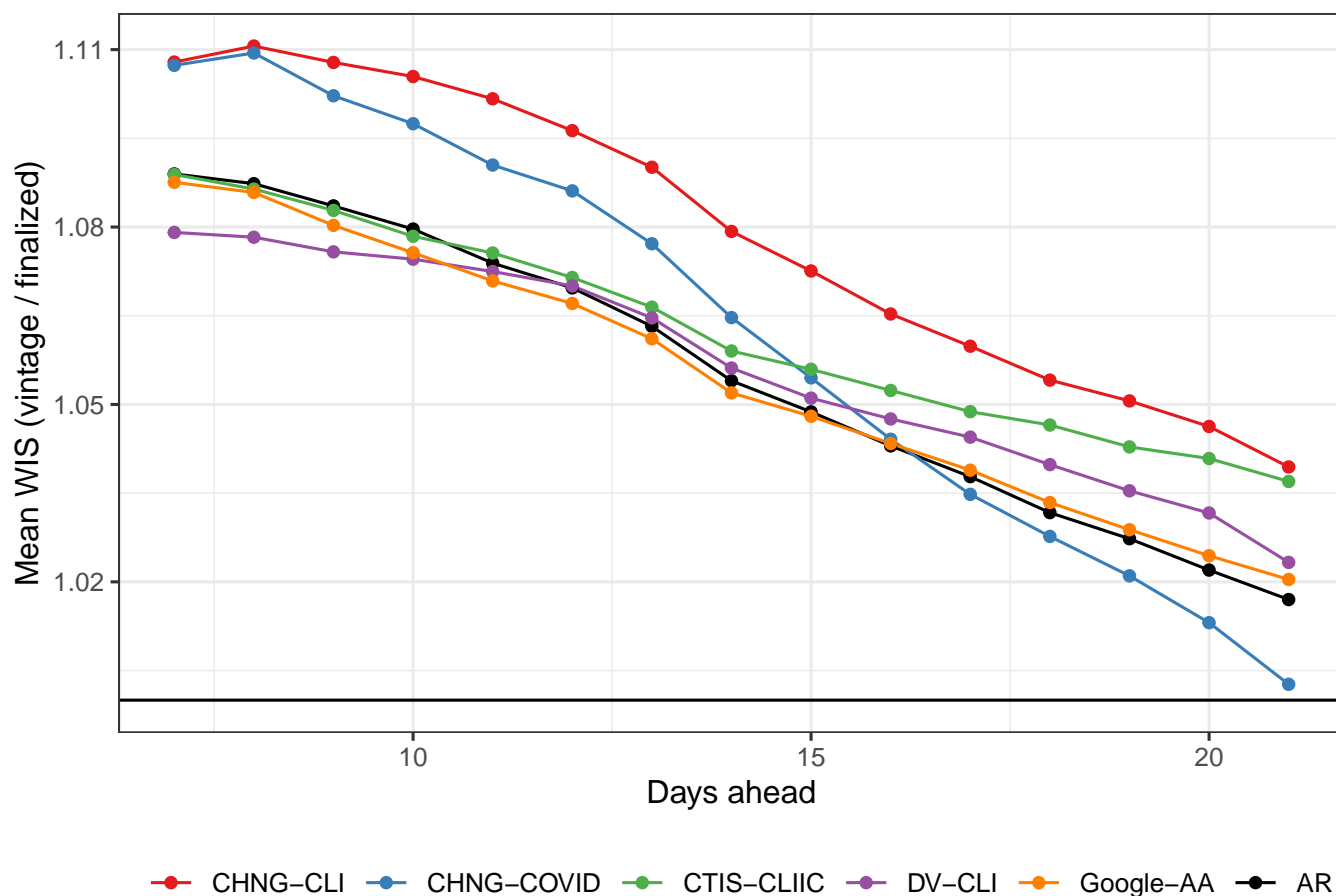


Fig. S3. Relative forecast WIS with vintage compared to finalized data. Using finalized data leads to overly optimistic performance.

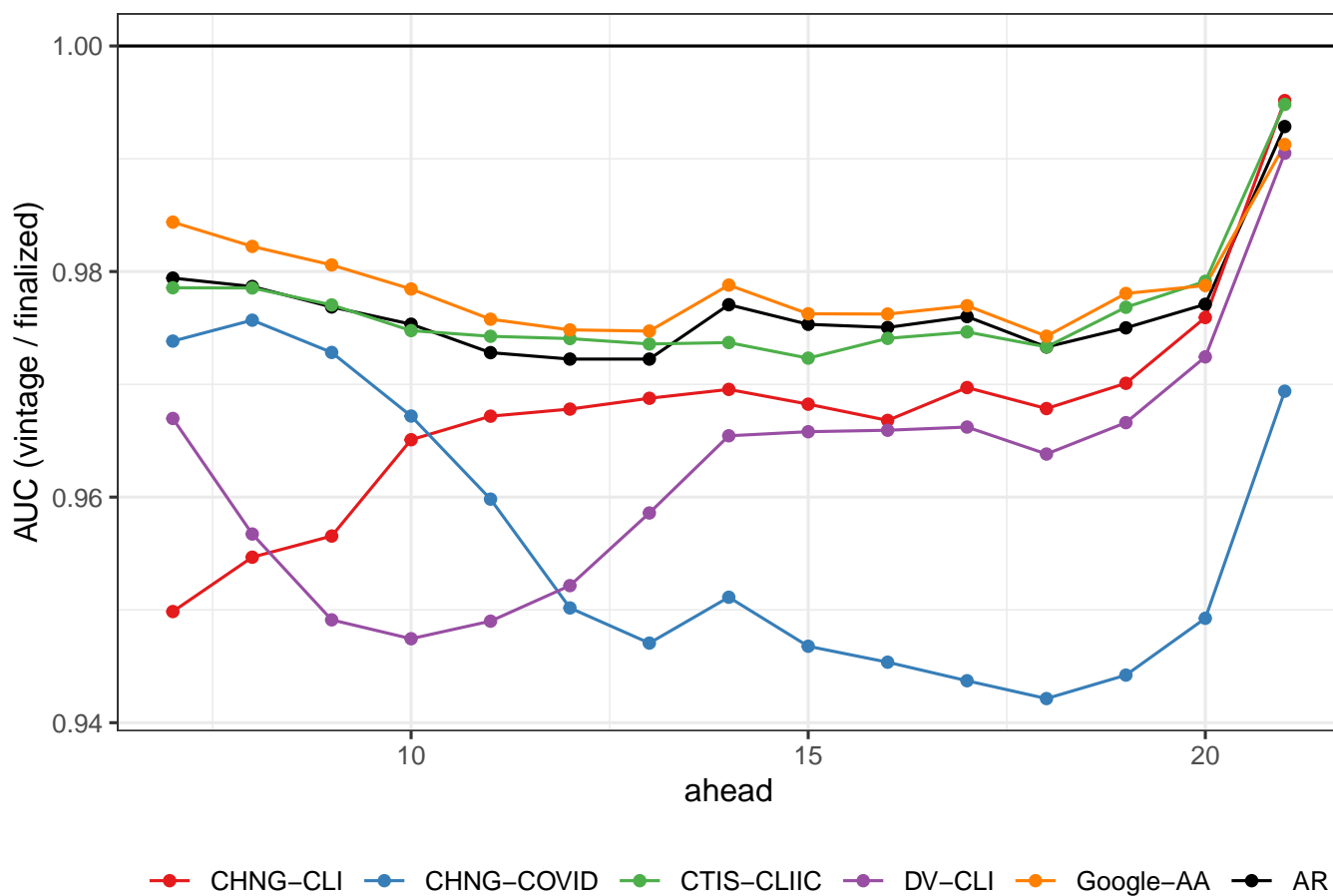


Fig. S4. Relative AUC with vintage compared to finalized data. Using finalized data leads to overly optimistic hotspot performance.

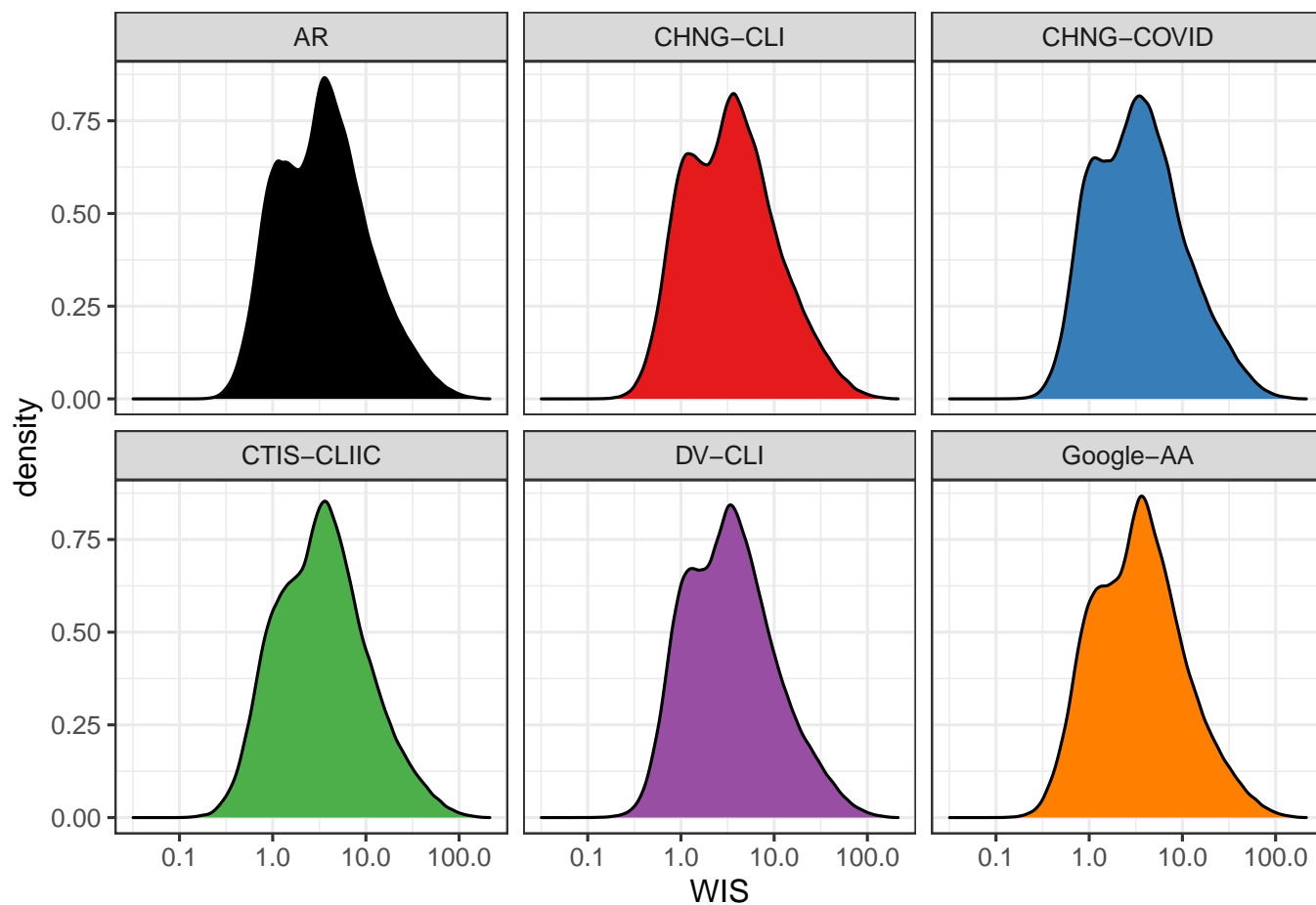


Fig. S5. Weighted interval score appears to more closely resemble a log-Gaussian distribution.

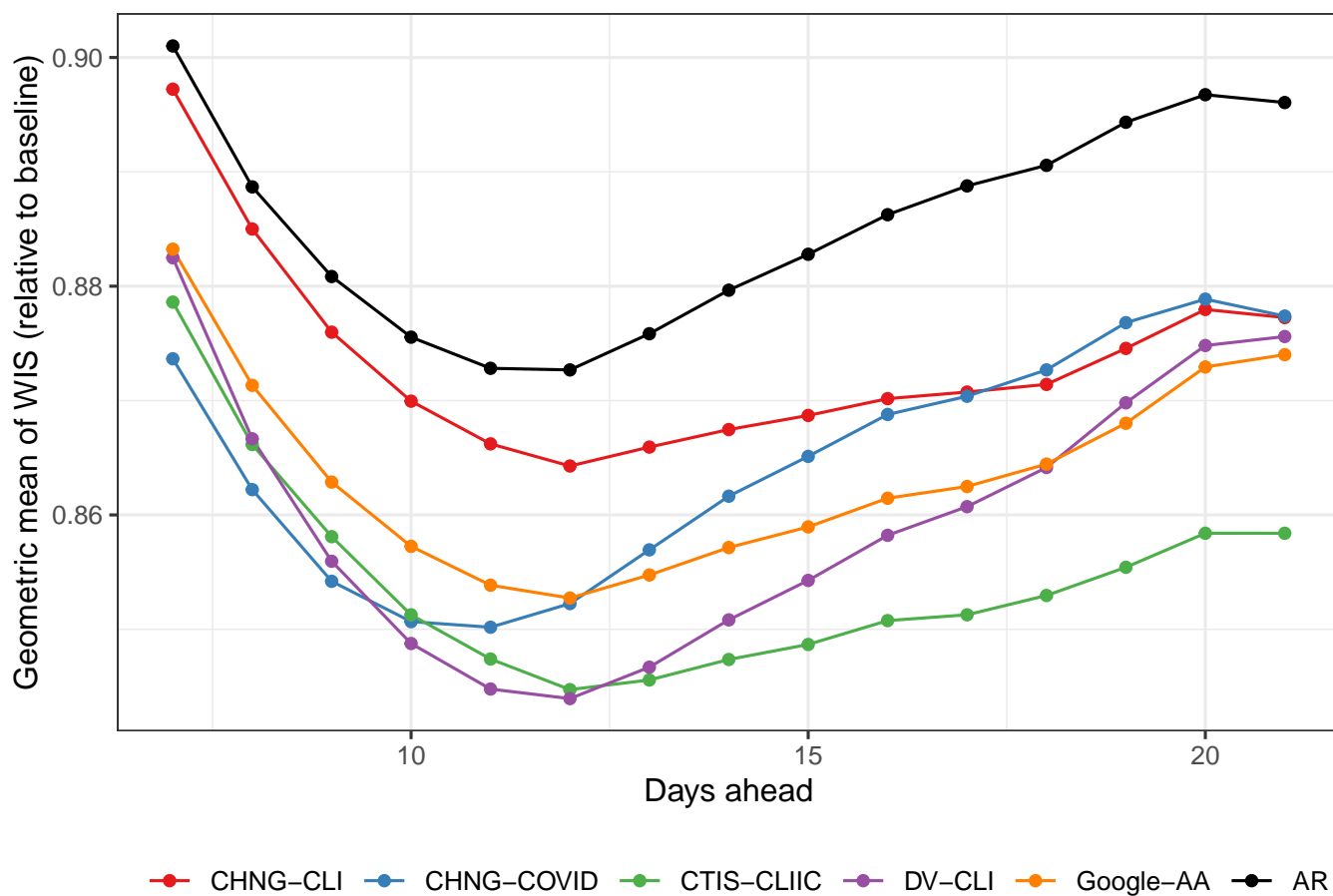


Fig. S6. Relative forecast performance using vintage data and summarizing with the more robust geometric mean.

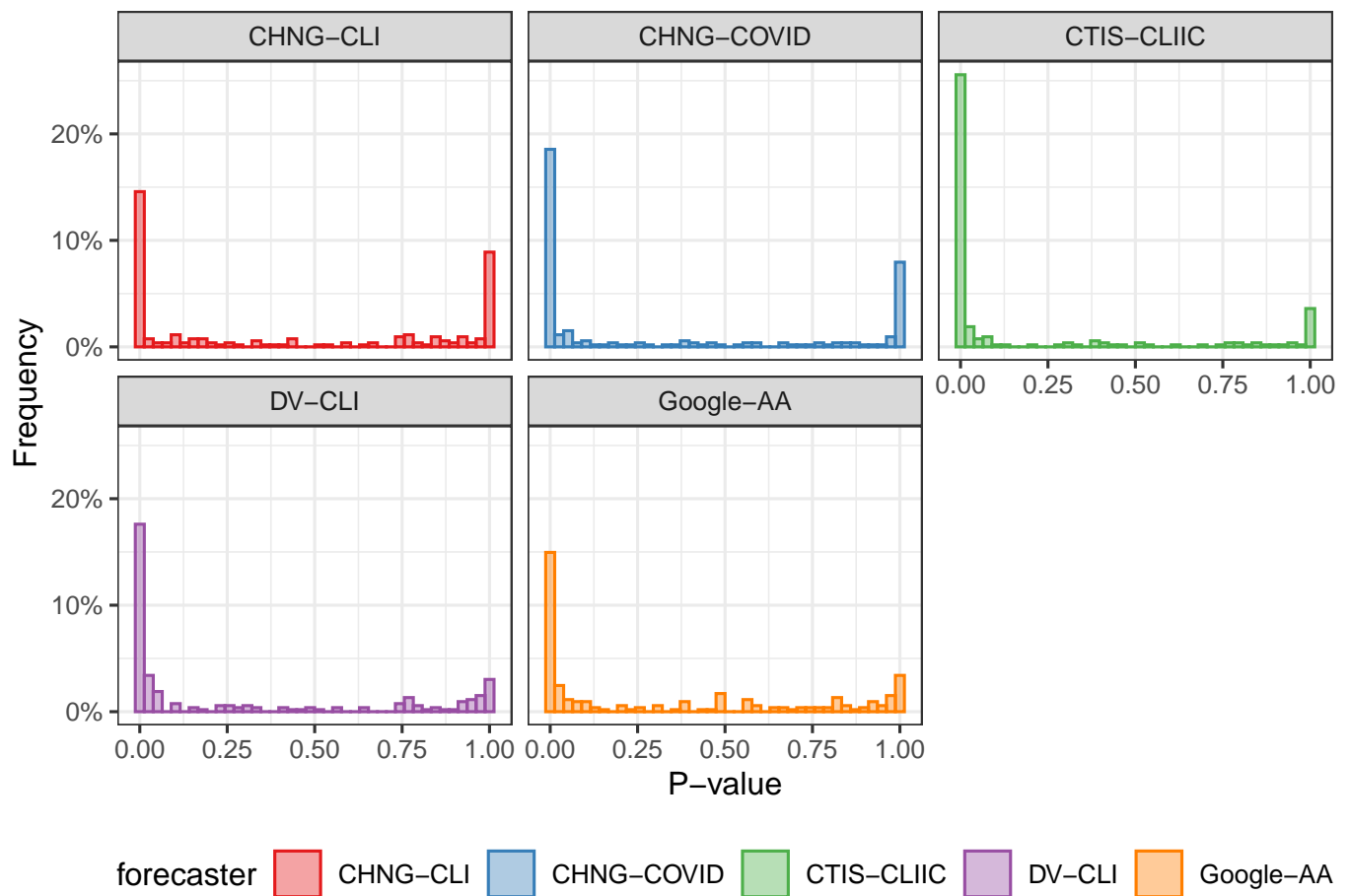


Fig. S7. P-values for a sign test that the WIS of the AR forecaster is smaller than that of the indicator-assisted model. Each P-value corresponds a particular forecast date.

Table S1. *P*-values for a one-sided Diebold-Mariano test for improvement in forecast error. The test is for the null hypothesis of equal performance against the alternative that the indicator assisted model is better.

metric	CHNG-CLI	CHNG-COVID	CTIS-CLIIC	DV-CLI	Google-AA
Geometric Mean Relative WIS	0.141	0.076	0.000	0.059	0.008
Mean Relative WIS	0.186	0.137	0.002	0.074	0.064

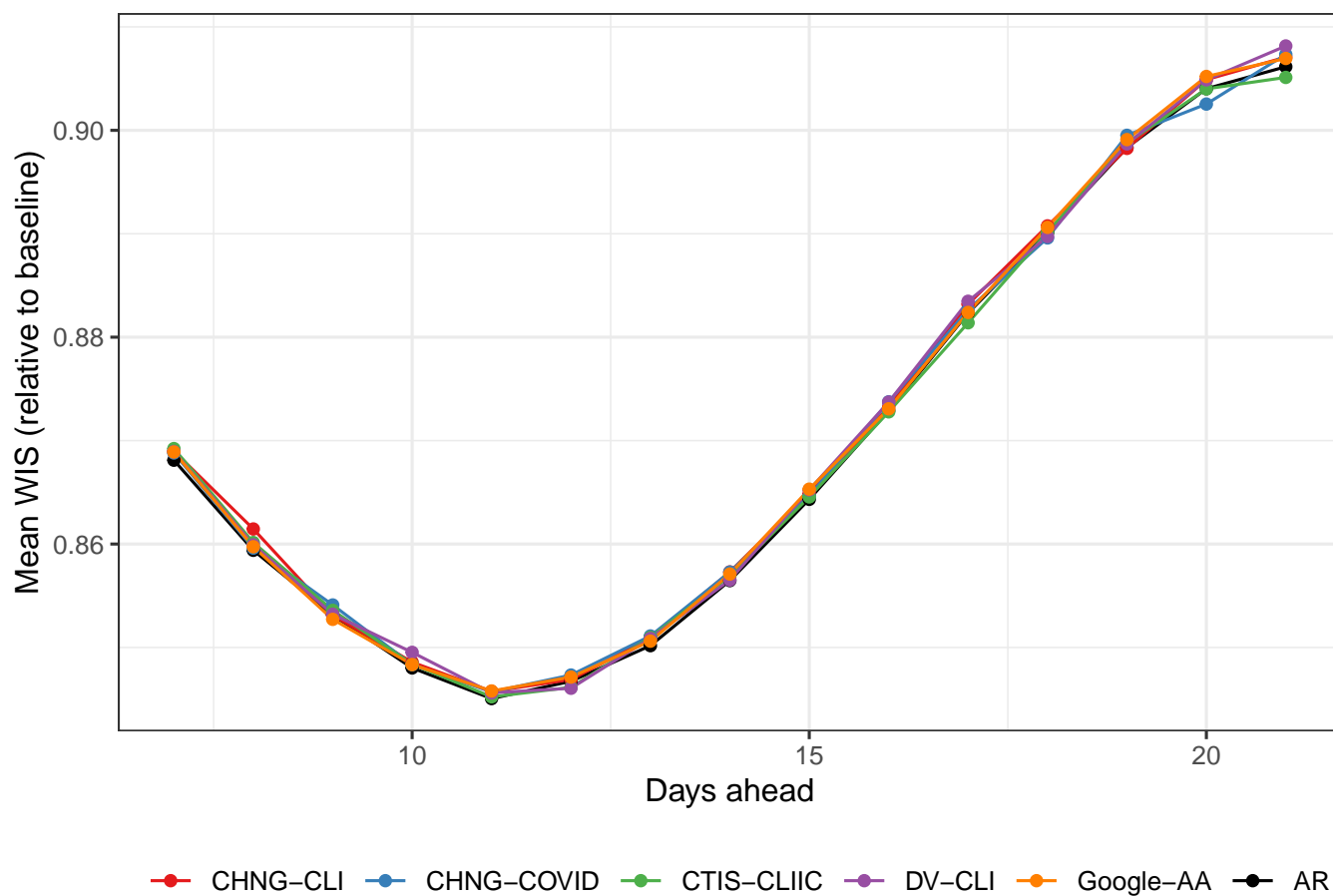


Fig. S8. Forecast performance when indicators are replaced with samples from their empirical distribution. Performance is largely similar to the AR model.

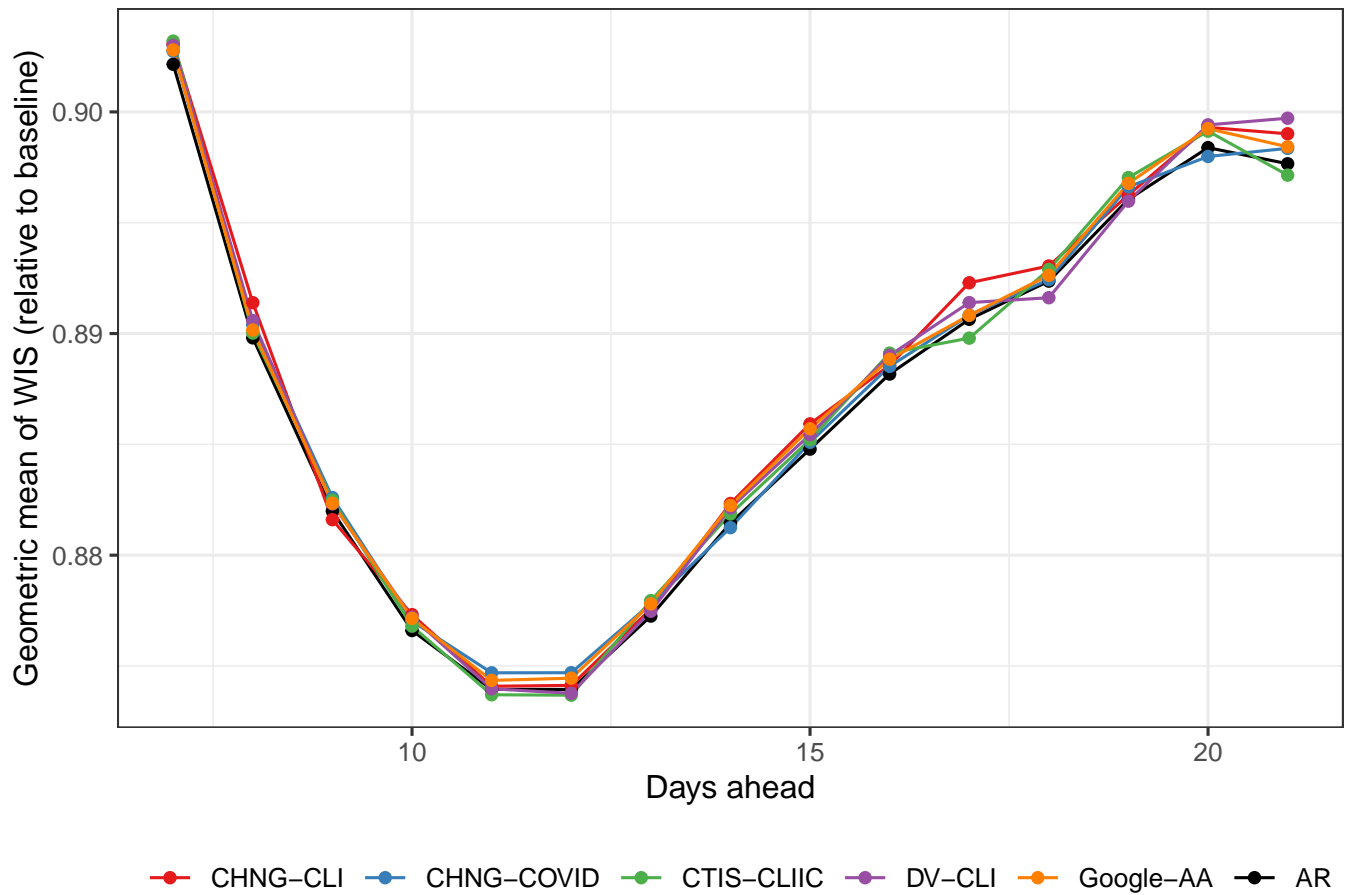


Fig. S9. Forecast performance as measured with the geometric mean when indicators are replaced with samples from their empirical distribution. Performance is largely similar to the AR model.

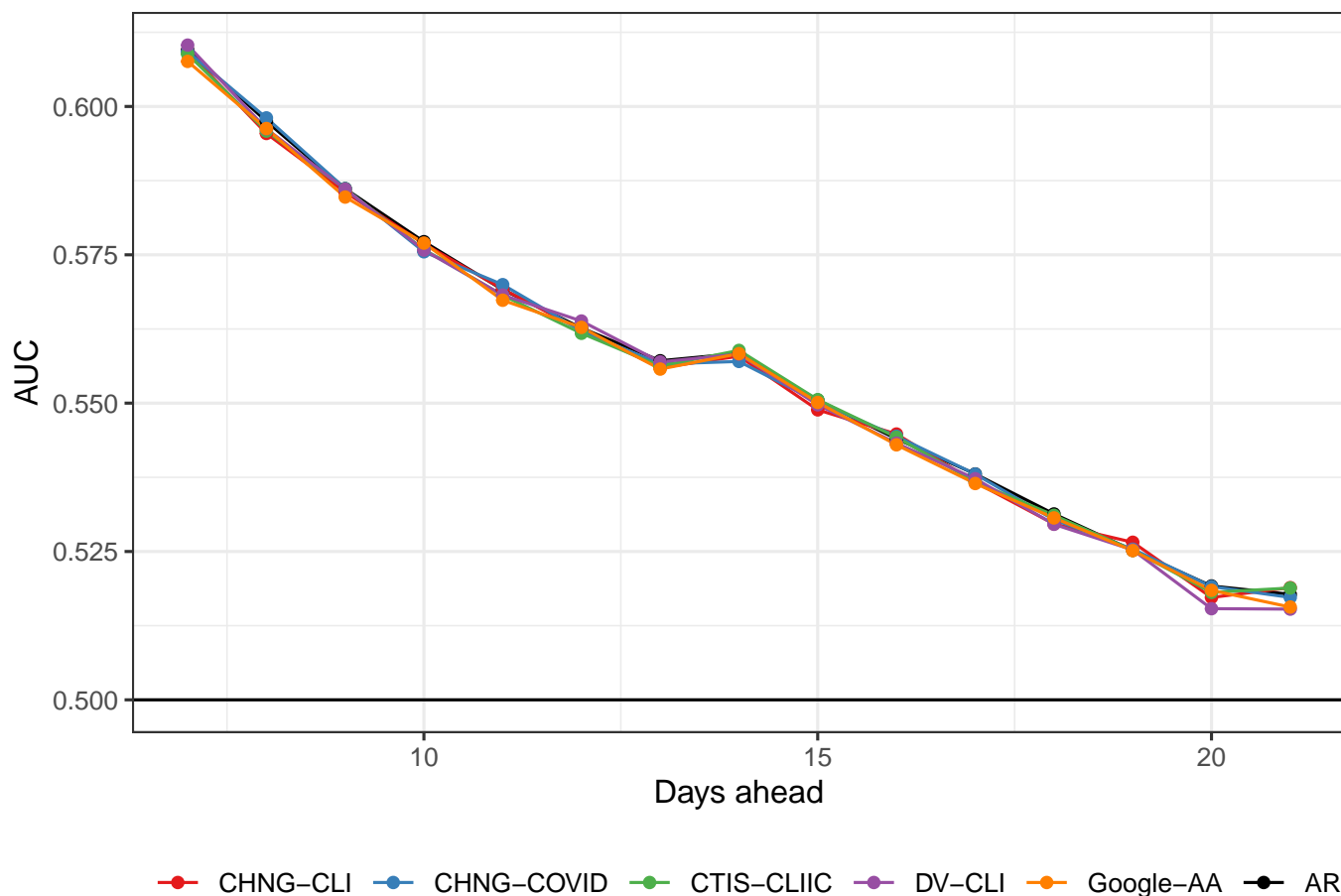


Fig. S10. Hotspot prediction performance when indicators are replaced with samples from their empirical distribution. Performance is largely similar to the AR model.

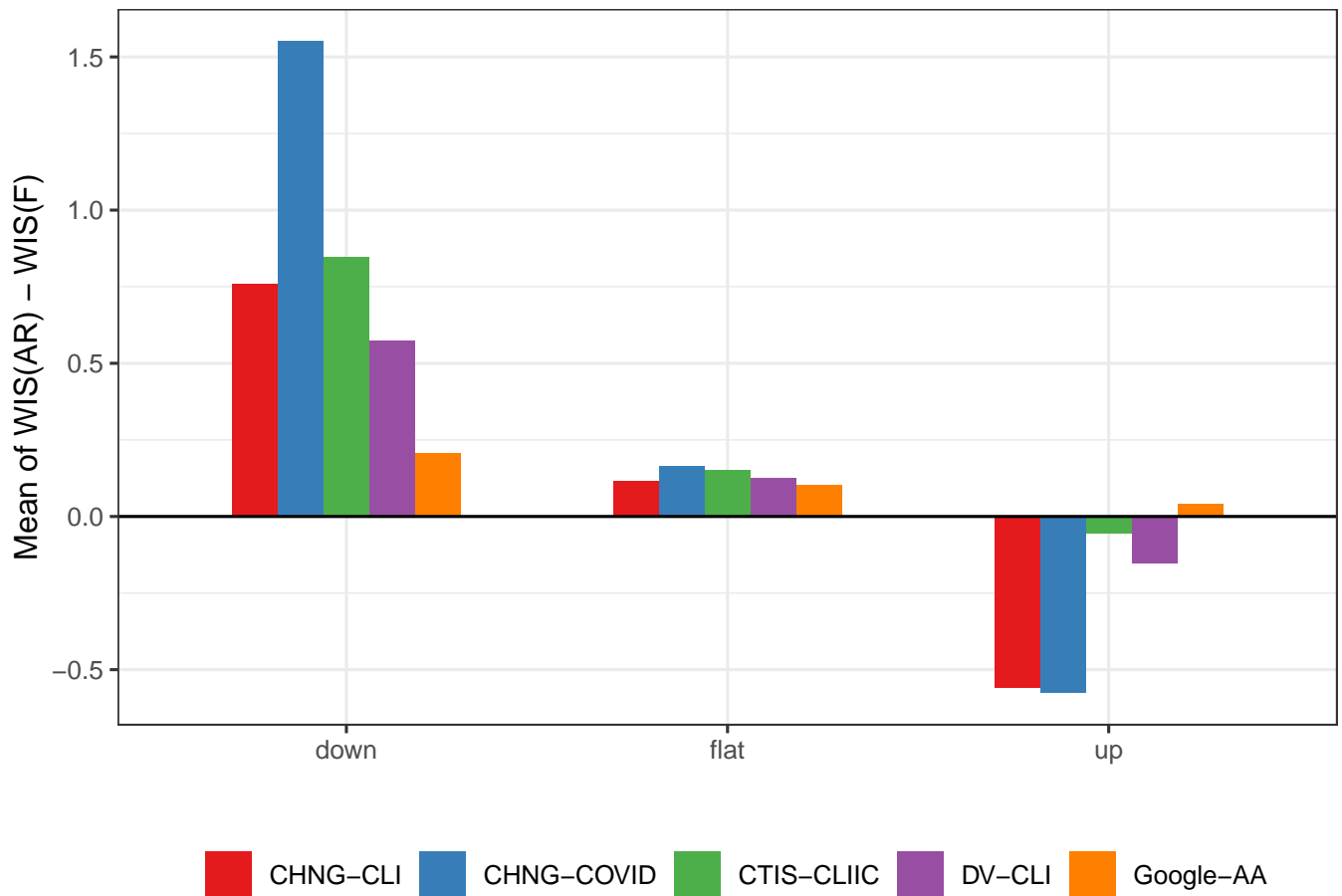


Fig. S11. Average difference between the WIS of the AR model and the WIS of the other forecasters. The indicator-assisted forecasters do best during down and flat periods.

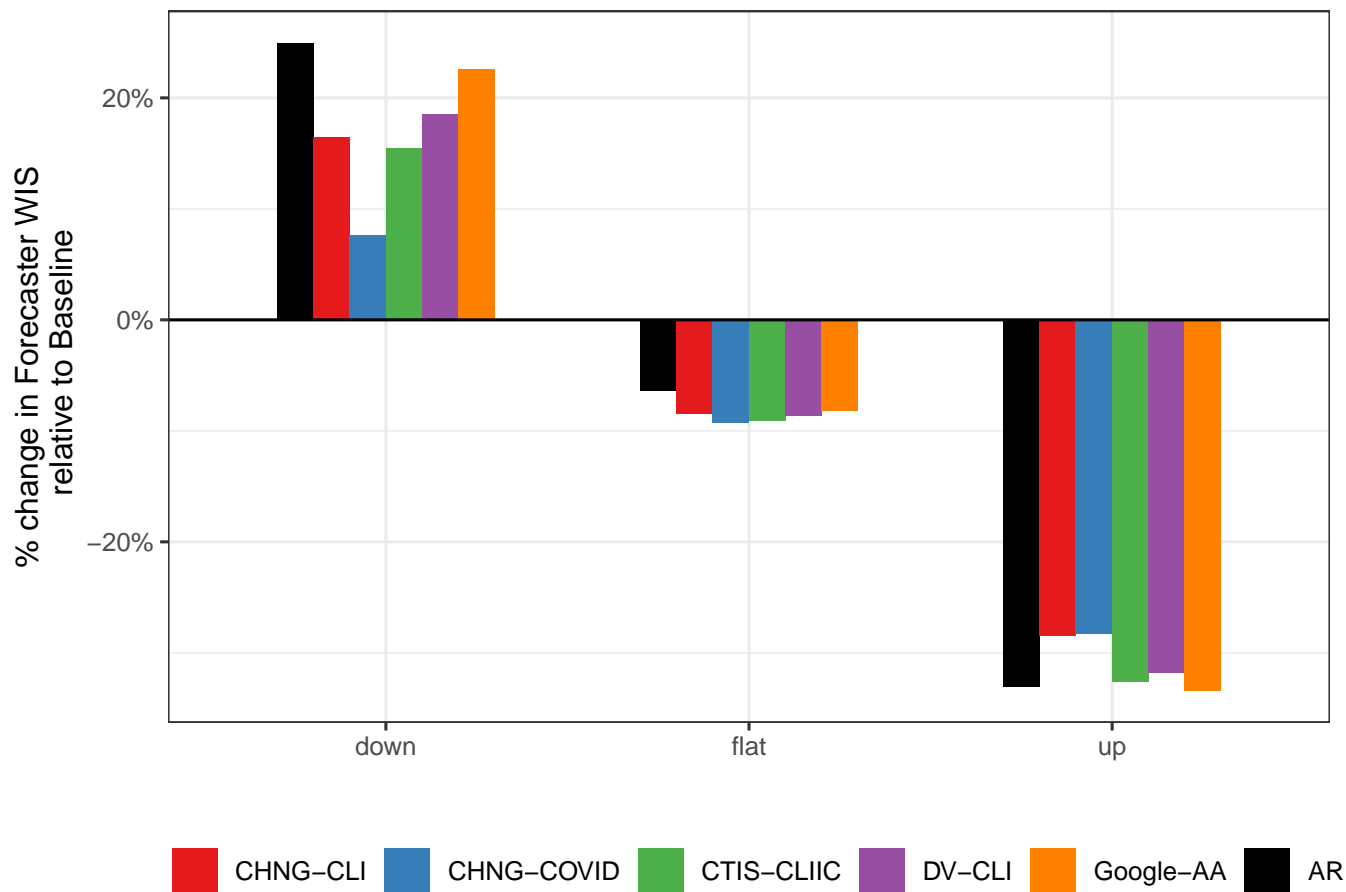


Fig. S12. REMAKE: Percent change in average WIS of the forecaster (AR or indicator assisted) relative to the baseline. All models perform poorly during down periods, but the indicators help. During flat periods, the indicators improve slightly over the AR. During up periods, all forecasters do much better than the baseline, but only some do as well as AR.

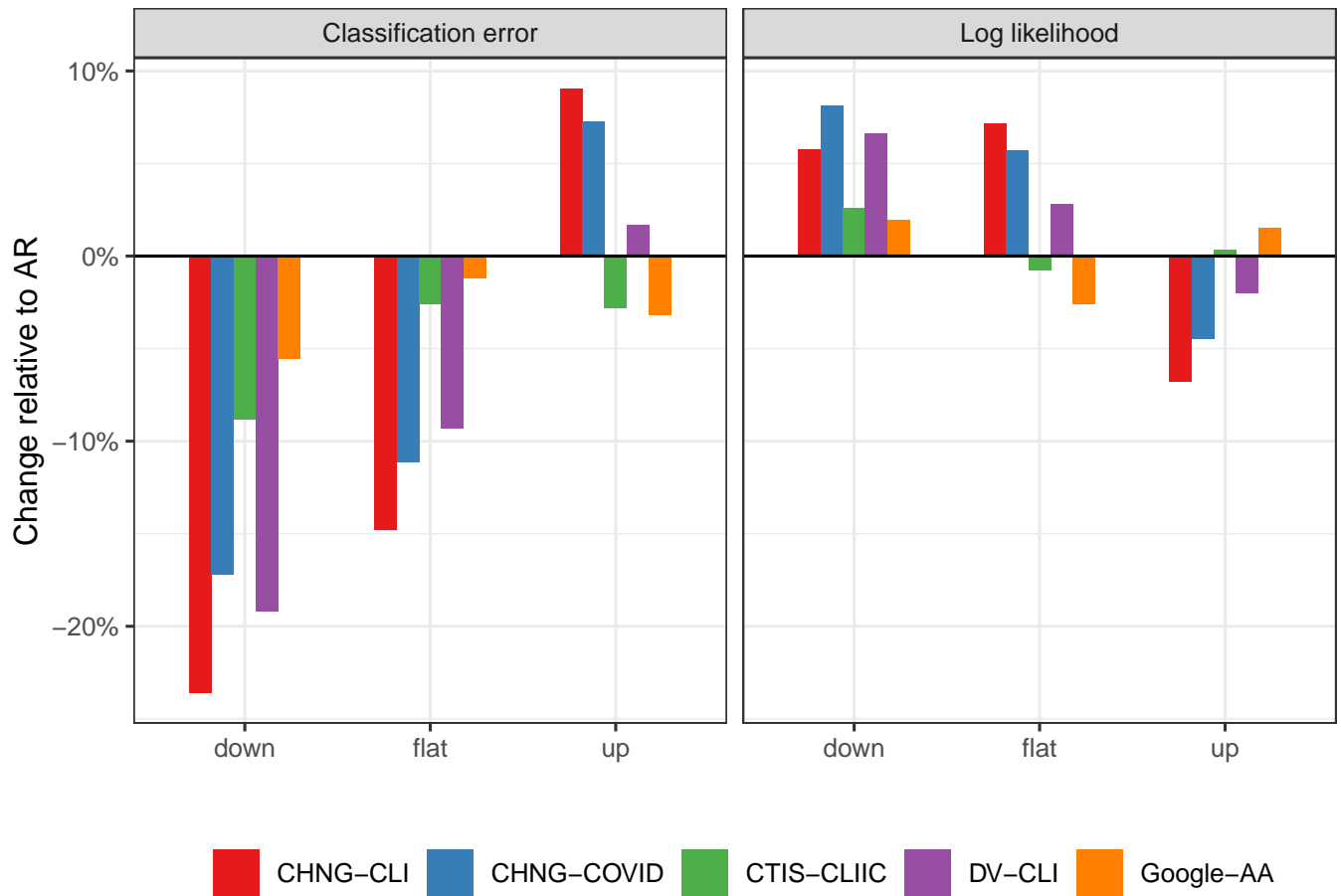


Fig. S13. Classification and loglikelihood separated into periods of upswing, downswing, and flat cases. Like the analysis of the forecasting task in the main paper (see Figure 7), performance is better during down and flat periods.

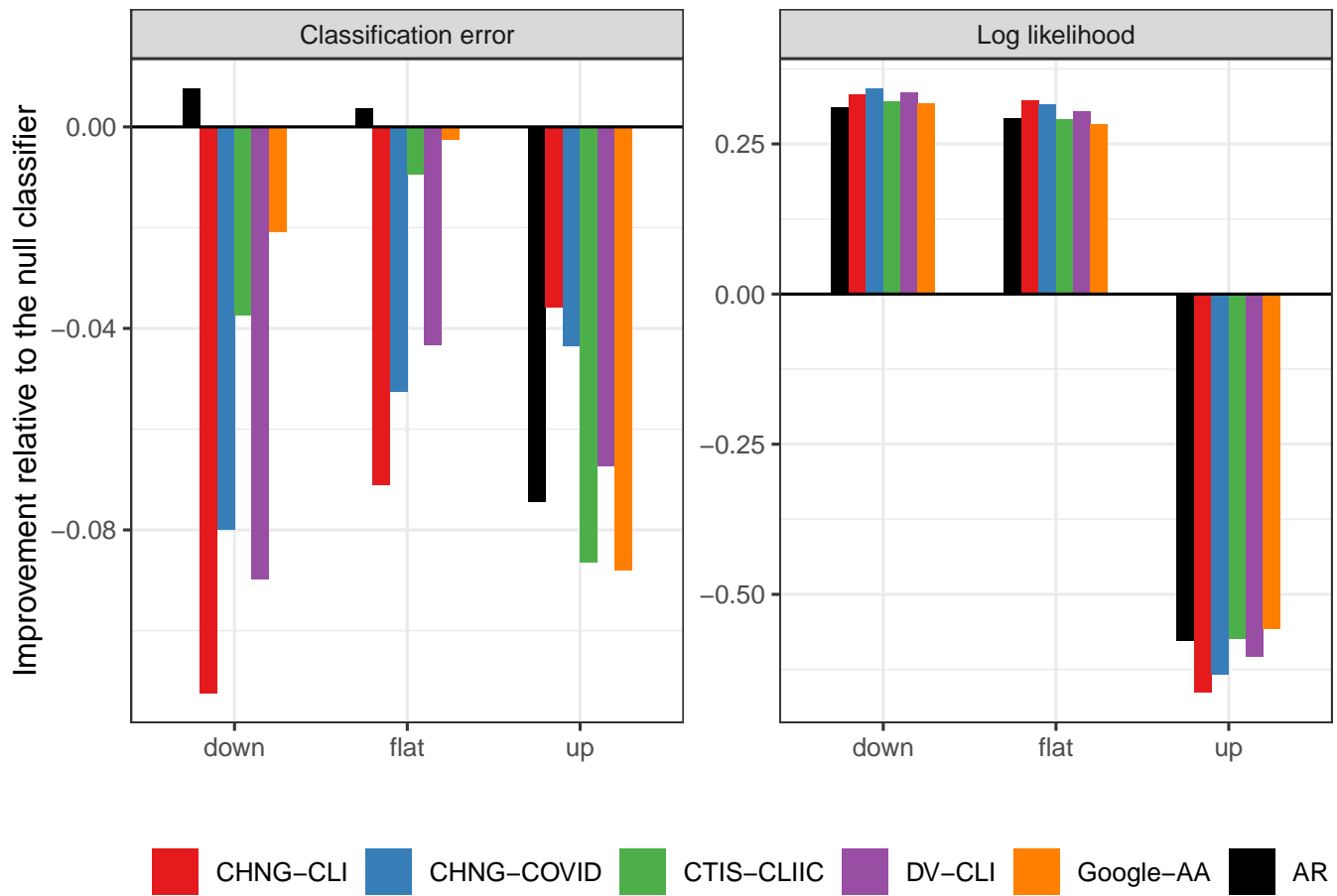


Fig. S14. REMAKE: Classification and loglikelihood separated into periods of upswing, downswing, and flat cases. The indicator assisted models always have lower classification error relative to the null classifier, while the AR actually does worse in down and flat periods. In terms of loglikelihood, all forecasters have lower likelihood than the null classifier during up periods. In down and flat periods, the indicators generally improve over the AR, while the are worse during up periods.

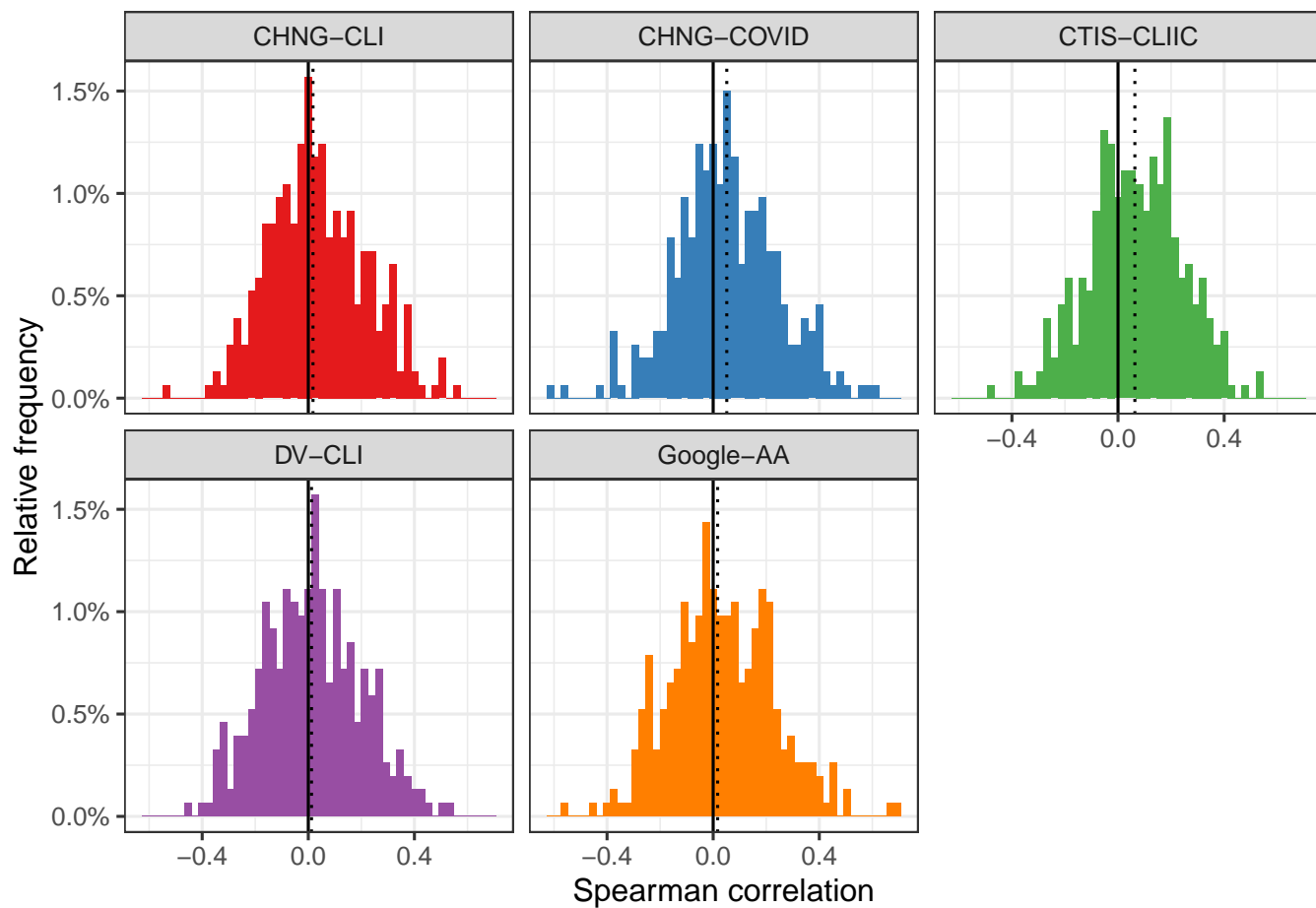


Fig. S15. Histograms of the Spearman correlation between the ratio of AR to AR WIS with the percent change in smoothed case rates relative to 7 days earlier.

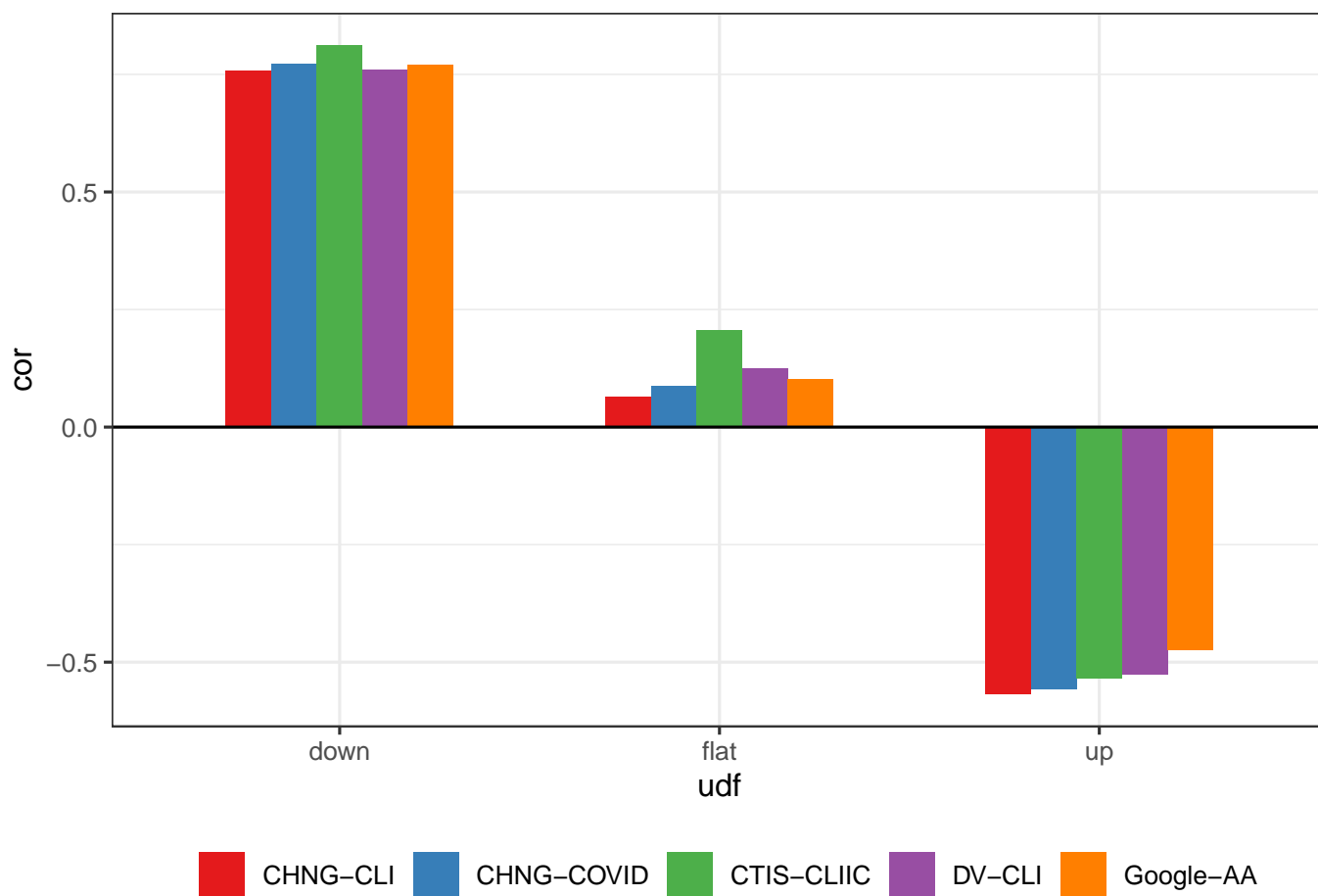


Fig. S16. Correlation of the difference in WIS with the difference in median predictions for the AR model relative to the indicator-assisted forecaster. In down periods, improvements in forecast risk are highly correlated with lower median predictions. The opposite is true in up periods. This suggests, as one might expect that improved performance of the indicator-assisted model is attributable to being closer to the truth than the AR model. This conclusion is stronger in down periods than in up periods.

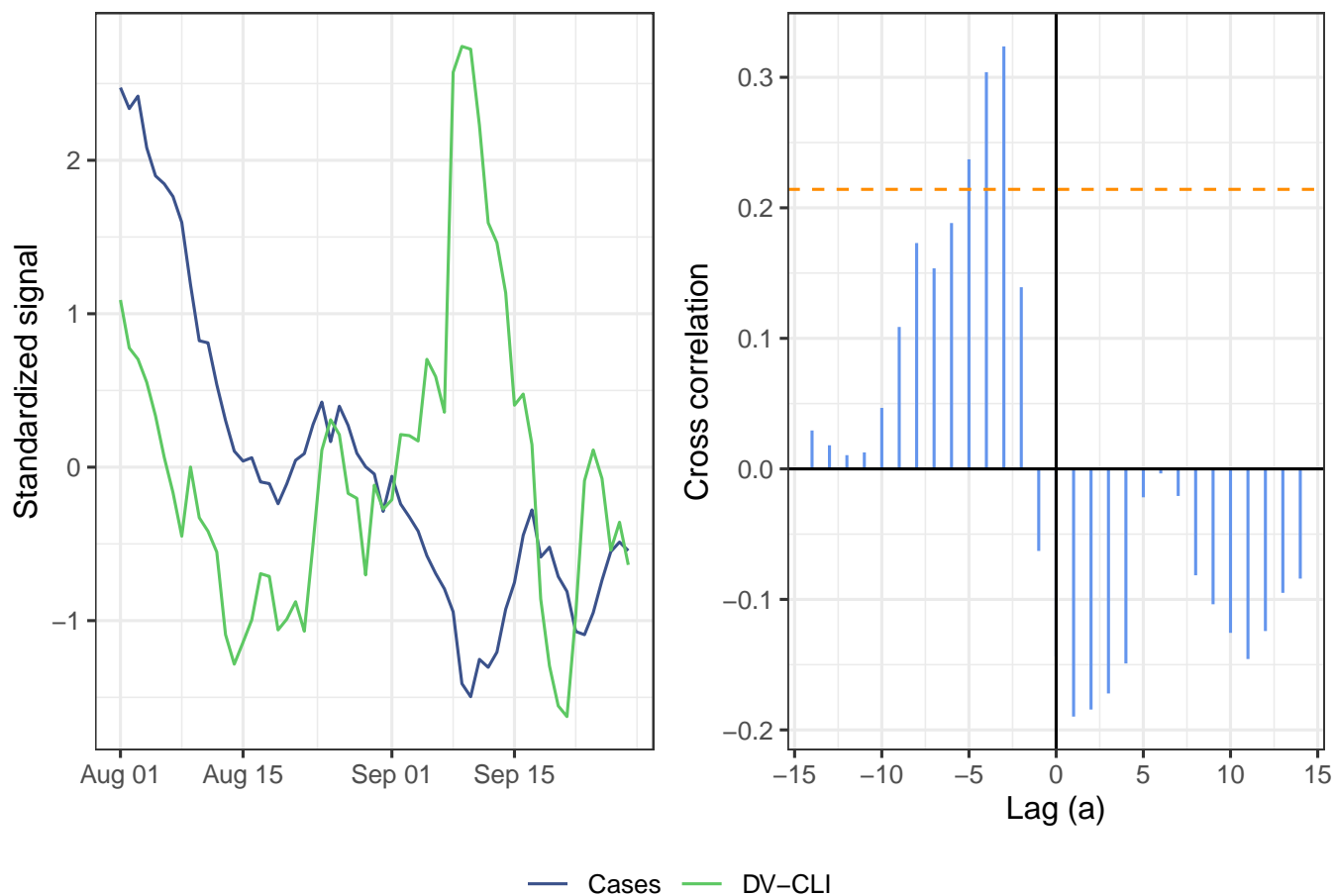


Fig. S17. Illustration of the cross-correlation function between DV-CLI and cases. The left panel shows the standardized signals over the period from August 1 to September 28 (as of May 15, 2021). The right panel shows $CCF_{\ell}(a)$ for different values of a as vertical blue bars. The orange dashed lines indicate the 95% significance threshold. By our leadingness/laggingness metric, DV-CLI is leading (but notlagging) cases over this period.

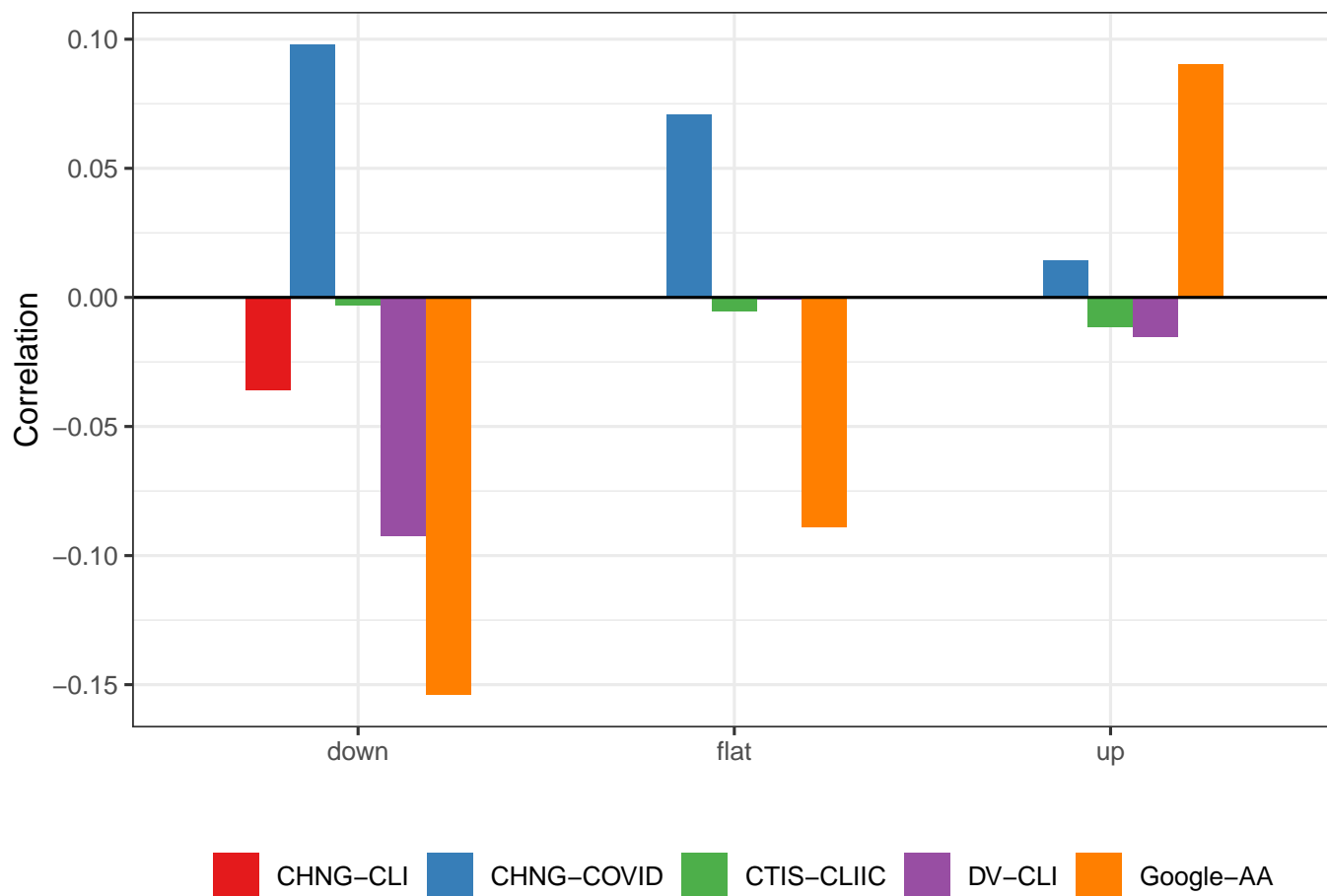


Fig. S18. Correlation of the difference in WIS with the laggingness of the indicator at the target date, stratified by up, down, or flat period. Compare to Figure 5 in the manuscript.

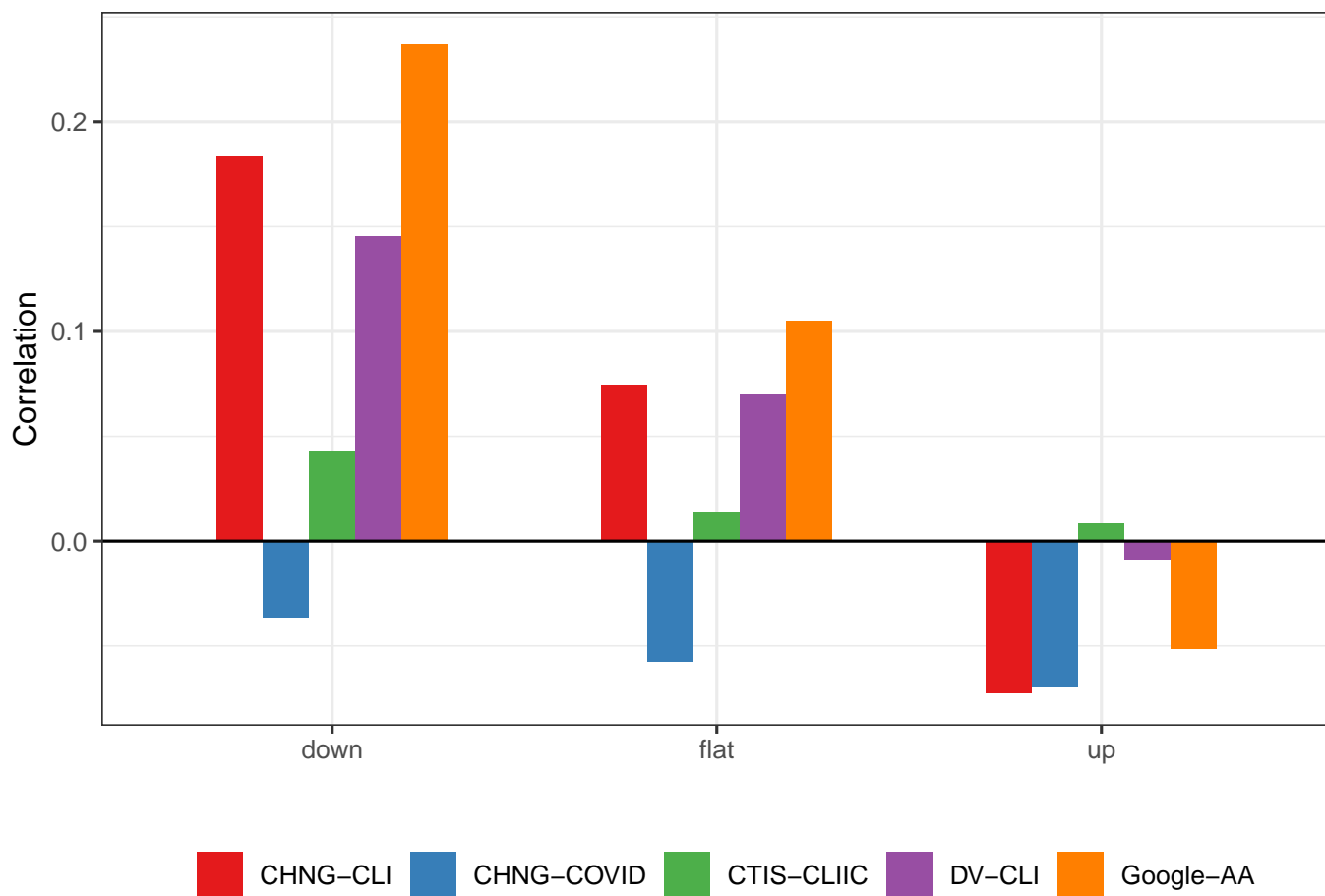


Fig. S19. Correlation of the difference between leadingness and laggingness with the difference in WIS. The relationship is essentially the same as described in the manuscript and shown in Figure 5.

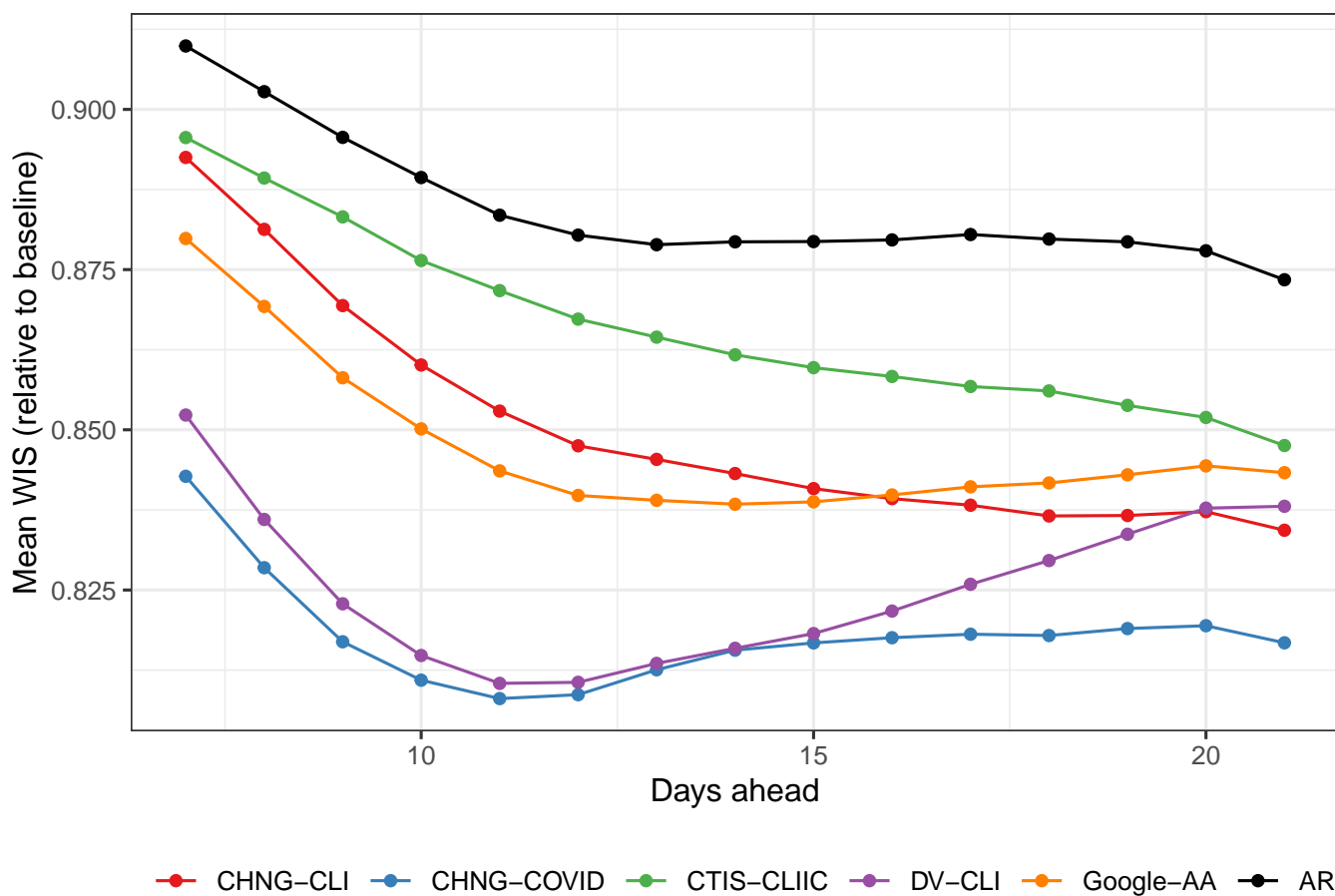


Fig. S20. Forecast performance over all periods. Performance largely improves for all forecasters with the inclusion of data in 2021.

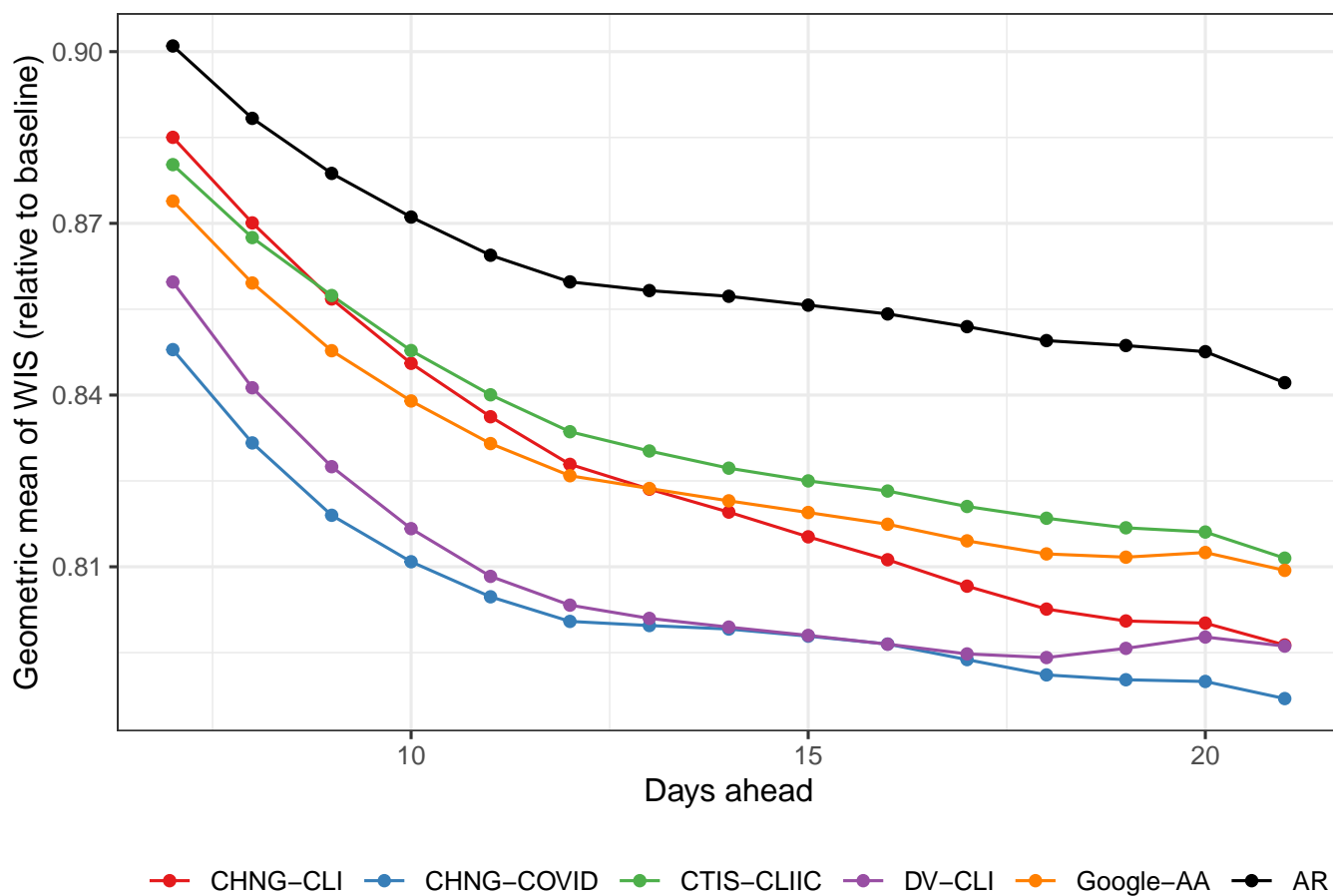


Fig. S21. Forecast performance over all periods aggregated with the geometric mean. Again, the inclusion of data in 2021 leads to improved performance.

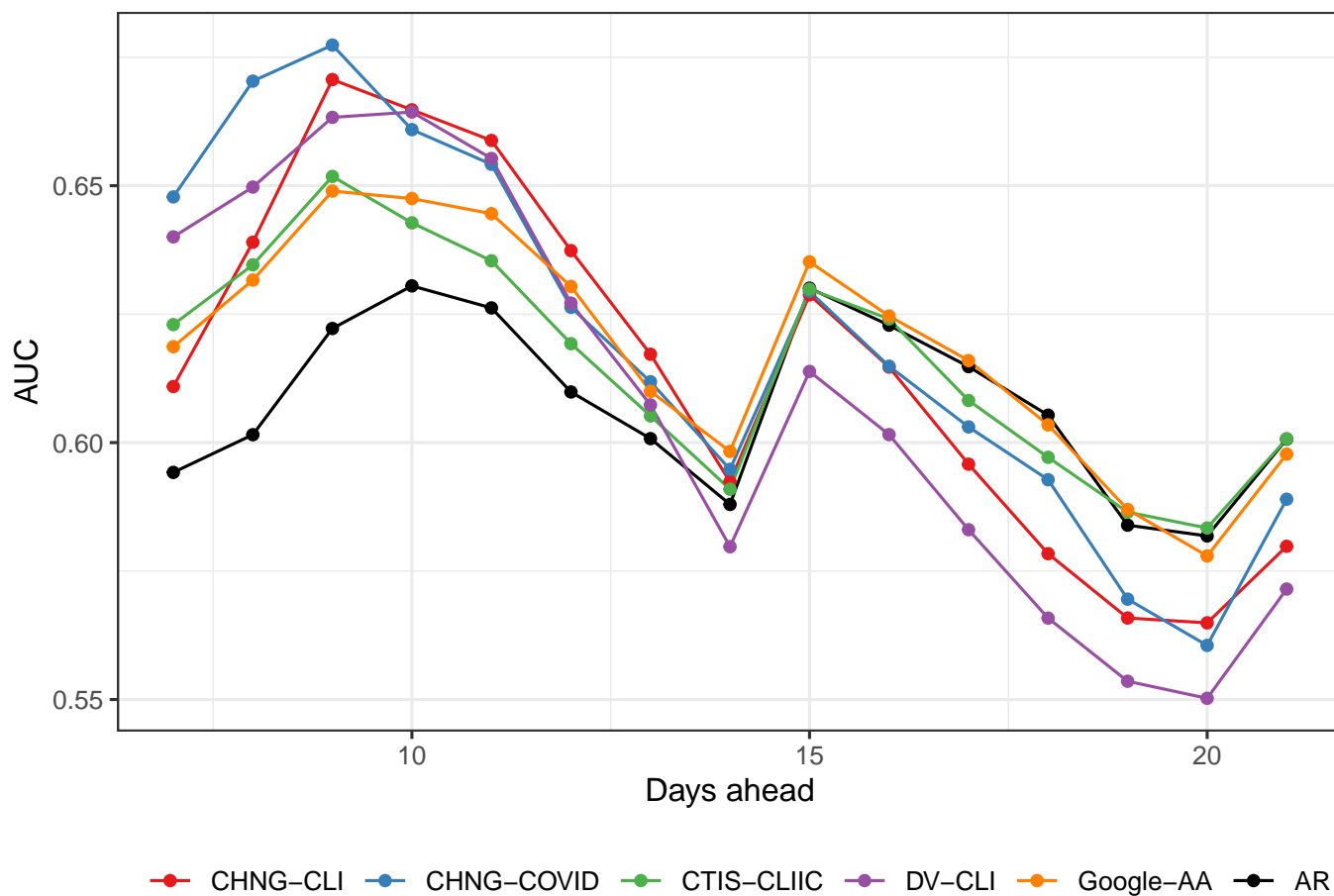


Fig. S22. Area under the curve for hotspot predictions including data in 2021. Performance degrades relative to the period in 2020. However, there are far fewer hotspots during this period as case rates declined in much of the country.

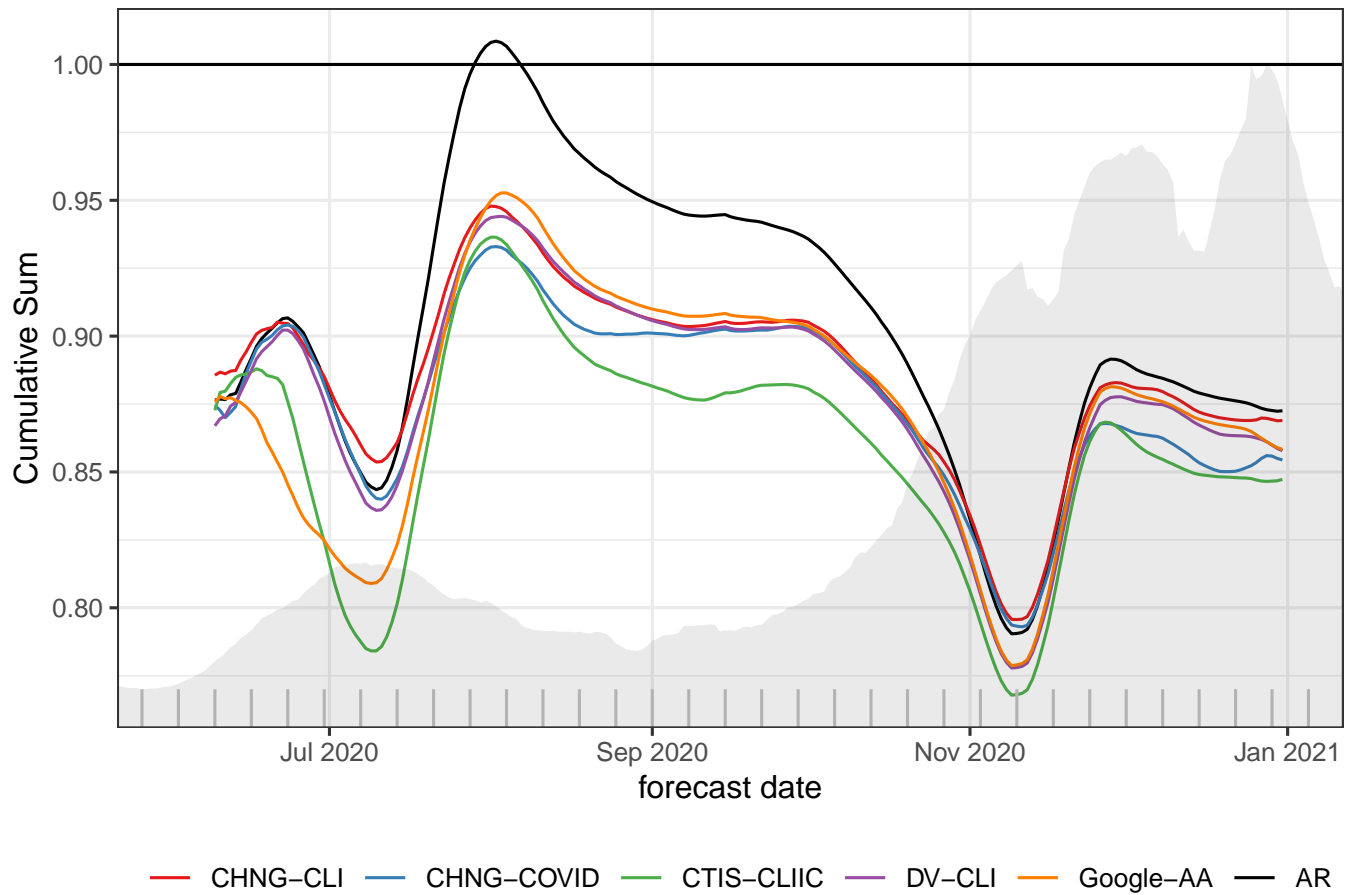


Fig. S23. This figure shows the cumulative sum of WIS for each forecaster divided by the cumulative sum of WIS for the baseline model. The shaded background shows total U.S. cases as reported by JHU-CSSE for the 14-day ahead target. Hashes along the x -axis denote weeks.

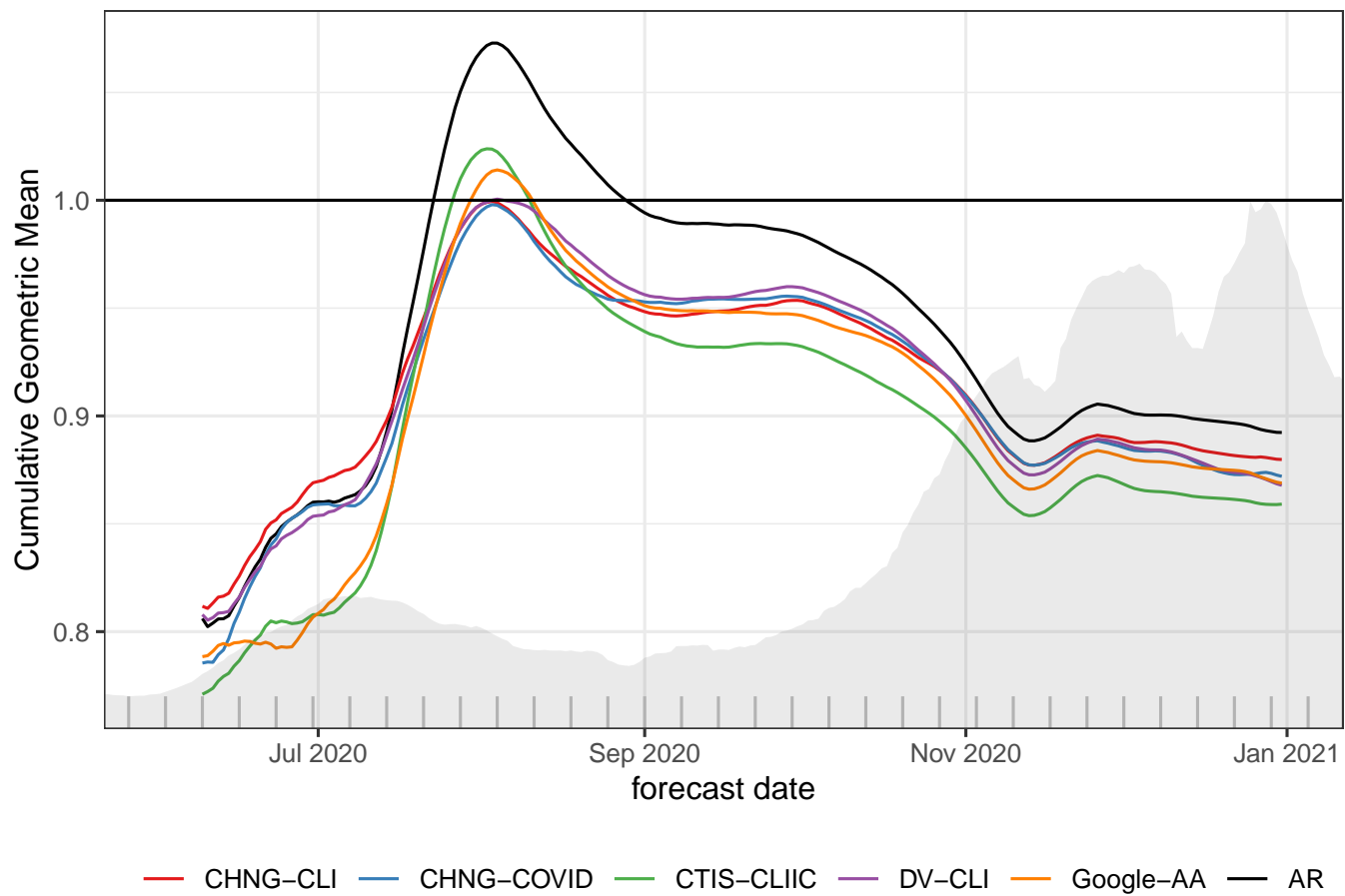


Fig. S24. This figure shows the cumulative geometric mean of WIS for each forecaster divided by the WIS for the baseline model. The shaded background shows total U.S. cases as reported by JHU-CSSE for the 14-day ahead target. Hashes along the x -axis denote weeks.

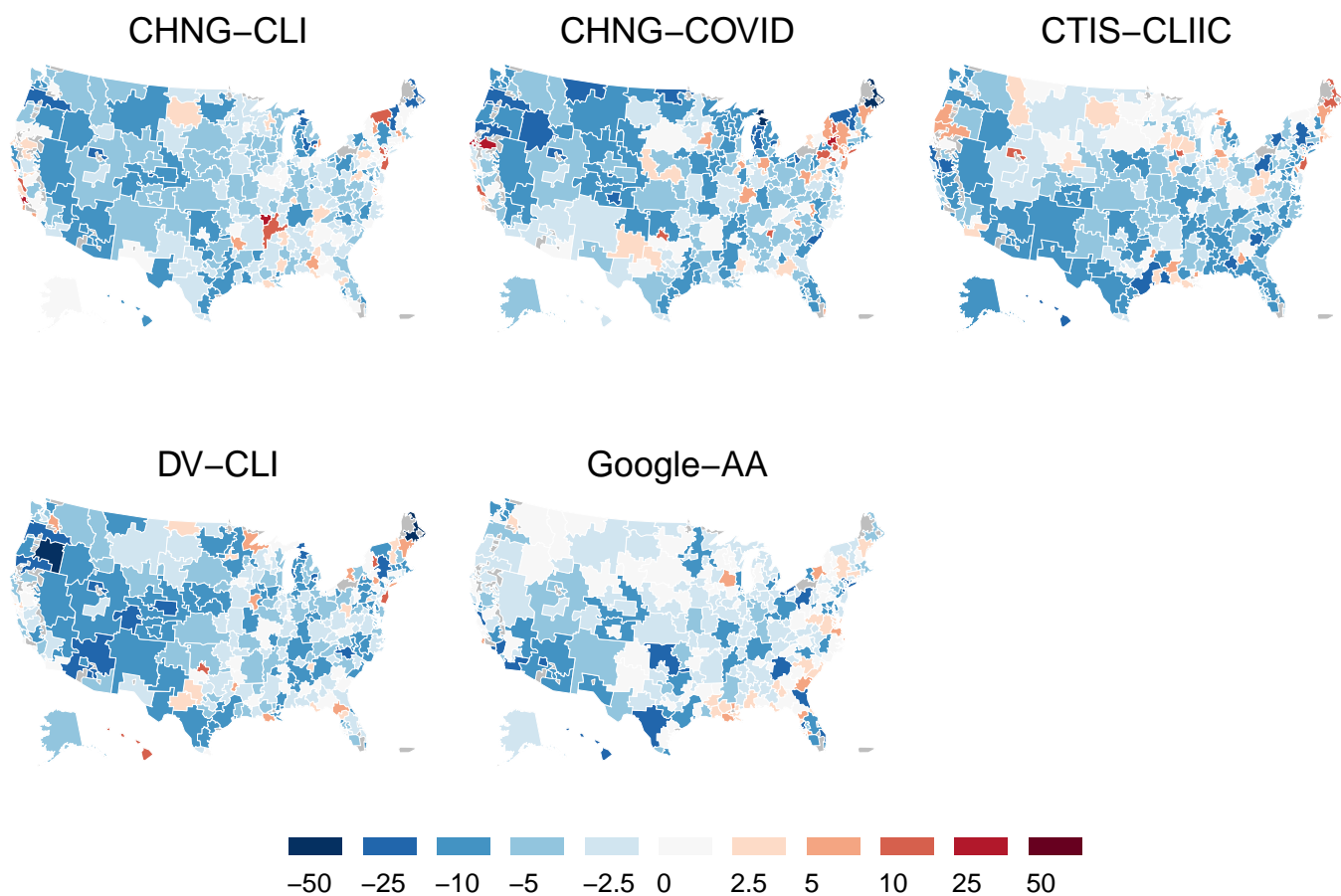


Fig. S25. Percent improvement in WIS relative to the AR forecaster by region (negative numbers indicate improved performance, positives indicate worsening).

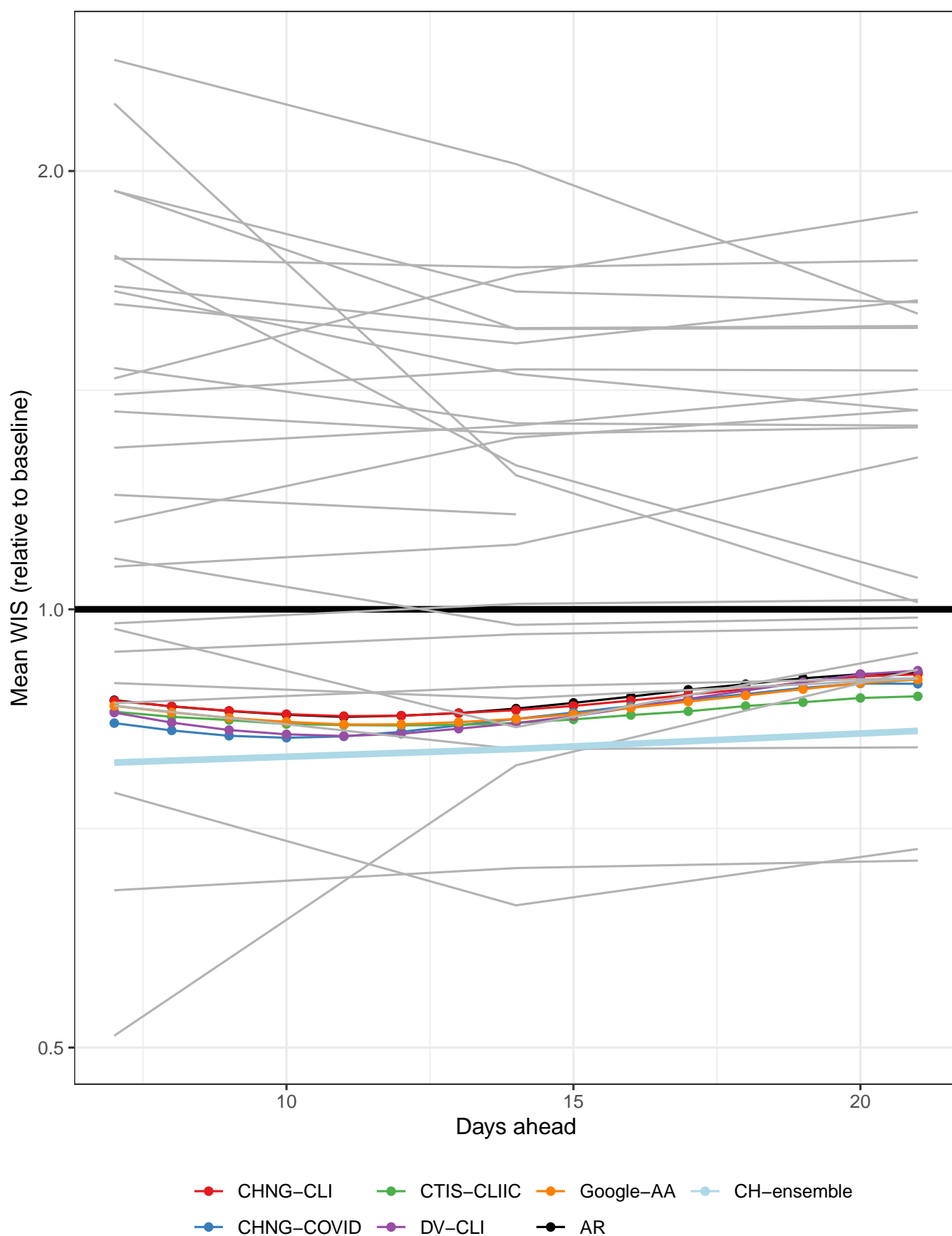


Fig. S26. This figure reproduces Figure 3 in the main paper but overlays scores for the forecasts submitted to the COVID-19 Forecast Hub. Grey lines correspond to the various teams that submitted during period our evaluation period. We have highlighted the COVIDhub-ensemble, which is the official forecast of the CDC.

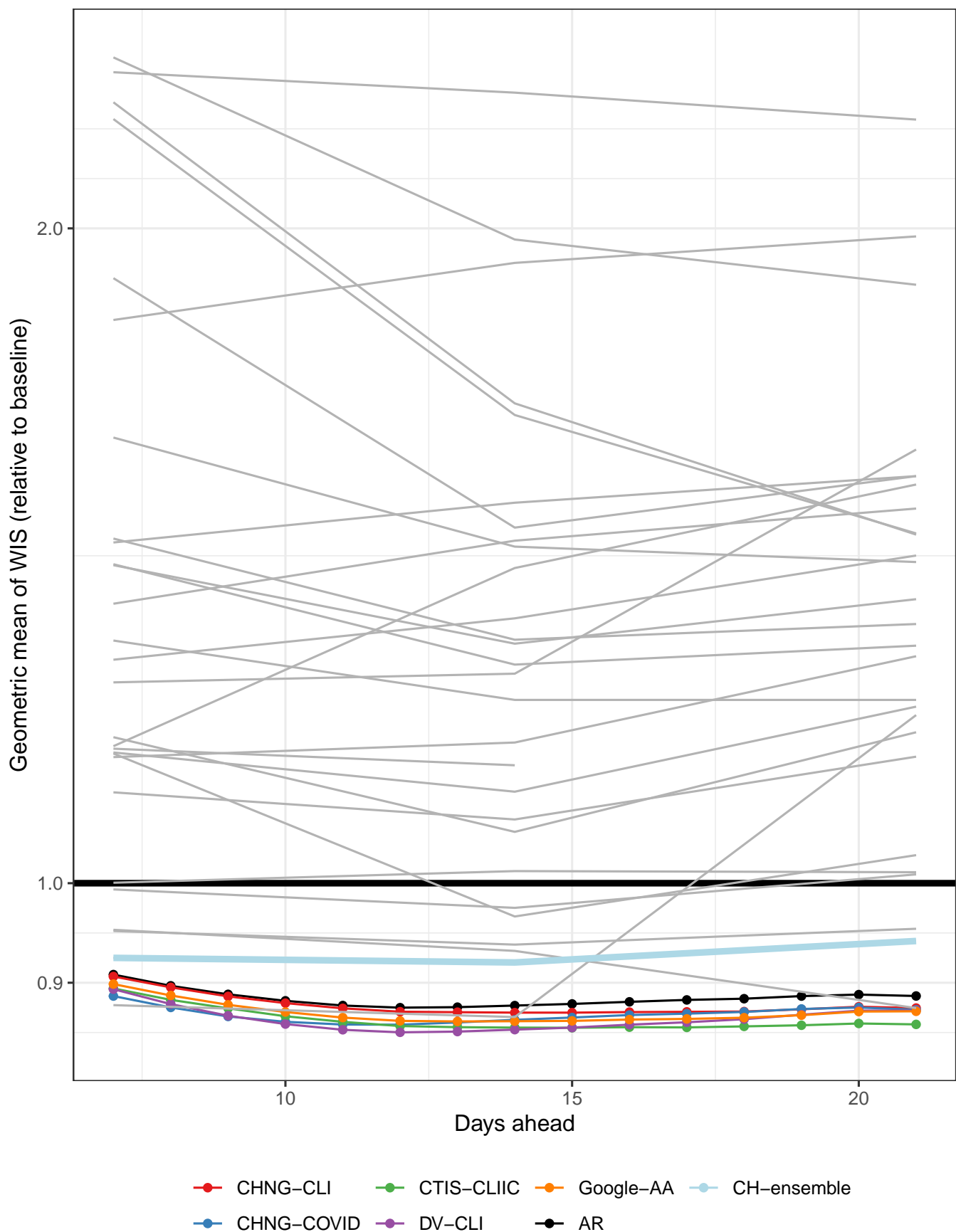


Fig. S27. This figure is similar to Figure S6. In this case, we add 1 to both the forecaster WIS and the baseline WIS before scaling (to allow forecasters that achieve 0 error to appear), and we overlay scores for the forecasts submitted to the COVID-19 Forecast Hub. Grey lines correspond to the various teams that submitted during period our evaluation period. We have highlighted the COVIDhub-ensemble, which is the official forecast of the CDC.

179 **SI Dataset S1 (predictions.zip)**
180 Archived .RDS (R objects) files containing all predictions for forecasting and hotspots using vintage and finalized data.
181 Persistent DOI to be added at publication.

182 **SI Dataset S2 (evaluations.zip)**
183 Archived .RDS (R objects) files containing all evaluations for forecasting and hotspots using vintage and finalized data.
184 Persistent DOI to be added at publication.

185 **SI Dataset S3 (analysis.zip)**
186 Archived .RDS (R objects) files containing additional data used to produce graphics and conclusions in the manuscript.
187 Persistent DOI to be added at publication.

188 **SI Dataset S4 (code.zip)**
189 R script files containing all code used to reproduce the analysis described in the manuscript. Persistent DOI to be added at
190 publication.

191 **References**

- 192 1 FX Diebold, RS Mariano, Comparing predictive accuracy. *J. Bus. & Econ. Stat.* **20**, 134–144 (2002).
- 193 2 FX Diebold, Comparing predictive accuracy, twenty years later: A personal perspective on the use and abuse of diebold–
194 mariano tests. *J. Bus. & Econ. Stat.* **33**, 1–24 (2015).
- 195 3 D Harvey, S Leybourne, P Newbold, Testing the equality of prediction mean squared errors. *Int. J. forecasting* **13**, 281–291
196 (1997).
- 197 4 Reich Lab, The COVID-19 Forecast Hub (<https://covid19forecasthub.org>) (2020).